UNIVERSITY OF GHANA

COLLEGE OF BASIC AND APPLIED SCIENCES

PLANNING TARGET MARGIN CALCULATIONS BASED ON THE EVALUATION OF ELECTRONIC PORTAL IMAGING DURING PROSTATE CANCER RADIOTHERAPY

BY

KAKAH, MAWUTOR YAOTSE

(10316077)

THIS THESIS/DISSERTATION IS SUBMITTED TO THE UNIVERSITY OF GHANA, LEGON

IN PARTIAL FULFILMENT OF THE REQUIREMENT FOR THE AWARD OF MPHIL MEDICAL PHYSICS DEGREE.

DEPARTMENT OF MEDICAL PHYSICS

SCHOOL OF NUCLEAR AND ALLIED SCIENCES

JULY, 2016

DECLARATION

This thesis is the result of research work undertaken by Kakah, Mawutor Yaotse in the Department of Medical Physics, School of Nuclear and Allied Sciences, University of Ghana, Legon. I hereby declare that this work contains no materials previously published by another person, nor material which has been presented for the award of any other degree of the School, except where due reference has been made in the text.

…… Date……

Kakah, Mawutor Yaotse

(Student's ID: 10316077)

……..……..... Date……..

Prof. J.H. Amuasi

(Principal supervisor)

…….. Date……

Dr. Stephen Inkoom

(Co-supervisor)

…… Date……..

Mr. Samuel Tagoe

(Co-supervisor)

ABSTRACT

Set-up errors are the inherent features of the radiation treatment process. Coverage of target volume is a direct function of set-up margins, which should be optimized to prevent unintended irradiation of adjacent normal tissues. The aim of this study was to evaluate three dimensional set-up errors and propose optimum margins for target volume coverage in prostate cancer radiotherapy. 1620 Portal images were obtained for an average of 30 fractions per patient for 54 prostate cancer patients. Electronic Portal Image (EPI) displacements obtained with iViewGT^{TM} imaging software along the three major axes (X, Y, Z) were analysed. Mean displacements, population systematic and random errors and

Three-dimensional vectors of displacements were calculated using StatPlus 2009 Professional 5.8.0 and Microsoft Excel (2013). Planning target margins were calculated using three different published margin recipes; the International Commission on Radiation Units and measurements (ICRU) 62, Stroom and van Herk. The random errors (σ) along vertical, lateral and longitudinal were 3.19 mm, 4.13 mm and 3.83 mm respectively. Similarly, the systematic errors (∑) were 1.81 mm, 2.83 mm and 2.51 mm along vertical, lateral and longitudinal axes respectively. The population mean (Mpop) displacement in vertical, lateral and longitudinal axes were -0.49 mm, 0.05 mm and -0.40 mm respectively and standard deviation in vertical, lateral and longitudinal axes were 3.75 mm, 5.20 mm and 4.76 mm respectively for the prostate cancer patients. Using ICRU report 62, the clinical target volume to planning target volume margins (CTV-PTV) were 3.67 mm, 5.00 mm and 4.58 mm along vertical, lateral and longitudinal axes respectively. The corresponding values were 5.85 mm, 8.54 mm and 7.69 mm with Stroom's formula whiles 3.75 mm, 6.96 mm and 5.95 mm were with van Herk's formula. The results suggest that there is a significant difference within the three major axes. Hence, the need for local departmental planning target margin protocol was recommended.

DEDICATION

I dedicate this work to Almighty God for His love, care, encouragement and protection He has given me throughout my education.

ACKNOWLEDGEMENTS

I am most grateful to God for His blessings and guidance that has made this work a reality. I am immensely indebted to my supervisors Prof. J.H. Amuasi, Dr. Stephen Inkoom and Mr. Samuel Nii Tagoe for their corrections and advice.

Special thanks to Mr. George F. Acquah and Mr. Philip Oppong Kyereme the Medical Physicists at Sweden Ghana Medical Centre for their assistance and advice offered me during this work.

TABLE OF CONTENTS

DECLARATION ii
ABSTRACT iii
DEDICATION iv
ACKNOWLEDGEMENT v
TABLE OF CONTENTS vi
LIST OF TABLES ix
LIST OF FIGURES xi
LIST OF ABBREVIATIONS xii
CHAPTER ONE 1
INTRODUCTION 1
1.1. Background 1
1.2. Statement of Problem 4
1.3. Aims and Objectives 4
1.4. Relevance and Justification 5
1.5. Scope and Limitation 5
1.6. Organisation of the Thesis 5
CHAPTER TWO 6
LITERATURE REVIEW 6
2.0. Introduction 6
2.1. Prostate anatomy 6
2.2. Dosimetry 9
2.2.1. Photon Fluence and Energy Fluence 11
2.2.2. Particle fluence ϕ 11
2.2.3. Energy Fluence (ψ) 12
2.2.4. Particle Fluence Rate ($\boldsymbol{\phi}$) 12
2.2.5. Energy fluence Rate $\boldsymbol{\psi}$ 12
2.2.6. Exposure X 13
2.2.7. Exposure Rate **X** 13
2.2.8. Absorbed Dose (D) 14
2.2.9. Integral Dose 15
2.2.10. Kerma (K) 15
2.2.11. Cema (C) 16
2.2.12. Organ Dose 17
2.2.13. Equivalent Dose (H_T) 17
2.2.14. Effective Dose 18

2.3. Techniques in Radiotherapy 19
2.3.1. Three Dimensional Conformal Radiation Therapy 19
2.3.2. Intensity Modulated Radiation Therapy 20
2.3.3. On Board Imaging and IGRT 20
2.3.4. Volumetric Modulated Arc Therapy (VMAT) 21
2.4. Dosimetric Characteristics of Radiation Beam 21
2.4.1. Radiation Beam Combination 23
2.5. Volume Delineation 25
2.5.1. Target Volumes 26
2.5.2. Organs at Risk 27
2.6. Organ Movement 28
2.7. Derivation of systematic and random set-up errors and relationship to the CTV-PTV margin. 29
2.7.1. Set-up error 29
2.7.2. Total population mean set-up error 30
2.7.3. Population systematic error 30
2.7.4. Random set-up errors 30
2.7.5. Individual Random Error 31
2.8. Margin derivation 31
CHAPTER THREE 33
MATERIALS AND METHODS 33
3.0. Introduction 33
3.1. Materials 33
3.1.1. Linear Accelerator 33
3.1.2. The iViewGT™ Electronic Portal Imaging Device 34
3.1.3. Treatment Planning System 35
3.2. Methods 36
3.2.1. Data Selection 36
3.2.2. Immobilization and Simulation using the CT 16 slice. 36
3.2.3. Portal Imaging and Analysis 37
3.2.4 Radiation Treatment Technique 38
3.3. Set-up Errors 39
3.3.1. Population Systematic Error 39
3.3.2. Population Random Errors 39
3.4. PTV Margin calculation 40
CHAPTER FOUR 41
RESULTS AND DISCUSSIONS 41

Results 41
4.0. Introduction 41
Discussions 52
4.1. Overview 52
4.2. Individual Mean and Total Population Mean. 53
4.2.1. Population Systematic (∑) and Random (σ) Errors 53
4.2.2. CTV-PTV Margin Calculation. 54
4.2.3. Scatter Plots in the three Displacements 54
4.2.4. Histogram in the three Directions 55
CHAPTER FIVE 56
CONCLUSIONS AND RECOMMENDATIONS 56
5.1. Conclusions 56
5.2. Recommendations. 57
5.2.1. Medical Physicists 57
5.2.2 Oncologists 57
5.2.3. Further Study 57
REFERENCES 58
APPENDIX A 63

LIST OF TABLES

Table 3. 1: Published CTV-PTV Margin Formulae.....40

Table 4. 1: Table of individual means, overall mean and systematic error in three directions.....41

Table 4. 2: Individual patient's random errors and overall mean of random errors. 44

Table 4. 3: The values of overall means, random errors and systematic errors.....47

Table A. 1: Individual set-up errors (Δ) acquired from patient 1-3.....63

Table A. 2: Individual set-up errors (Δ) acquired from patient 4-6.....64

Table A. 3: Individual set-up errors (Δ) acquired from patient 7-9.....65

Table A. 4: Individual set-up errors (Δ) acquired from patient 10-12.....66

Table A. 5: Individual set-up errors (Δ) acquired from patient 13-15.....67

Table A. 6: Individual set-up errors (Δ) acquired from patient 16-18.....68

Table A. 7: Individual set-up errors (Δ) acquired from patient 19-21.....69

Table A. 8: Individual set-up errors (Δ) acquired from patient 21-24.....70

Table A. 9: Individual set-up errors (Δ) acquired from patient 25-27.....71

Table A. 10: Individual set-up errors (Δ) acquired from patient 28-30.....72

Table A. 11: Individual set-up errors (Δ) acquired from patient 31-33.....73

Table A. 12: Individual set-up errors (Δ) acquired from patient 34-36.....74

Table A. 13: Individual set-up errors (Δ) acquired from patient 37-39.....75

Table A. 14: Individual set-up errors (Δ) acquired from patient 40-42.....76

Table A. 15: Individual set-up errors (Δ) acquired from patient 43-45.....77

Table A. 16: Individual set-up errors (Δ) acquired from patient 46-48.....78

Table A. 17: Individual set-up errors (Δ) acquired from patient 49-51.....79

Table A. 18: Individual set-up errors (Δ) acquired from patient 52-54. 80

LIST OF FIGURES

Figure 2.1: Sagittal view of male pelvic anatomy. From [42] 7

Figure 2.2: A schematic diagram of an Elekta treatment head [39]…..…….8

Plate 3. 1: State –of- art Linear Accelerator at Sweden Ghana Medical centre……34

Figure 2. 3: Regions of relative predominance for the three main forms of photon interactions with matter for different atomic numbers Z and photon energies. From [41] 10

Figure 2. 4: a) Central axis depth dose curves of multiple beam energies [16]. (b) Typical Co-60 beam profile. c) Typical 6MV isodose chart [17]. (a) and (b) taken from Khan [16], (c) taken from Karzmark et al [17]. 23

Figure 2. 5: Combination of posterior and anterior fields to produce parallel opposed dose distribution [1]. 24

Figure 2. 6: Dose distribution for four field box technique [1] 25

Figure 2. 7: Delineation of PTV by the teacher, students and the groups at ESTRO teaching course..... 26

Figure 2. 8: ICRU Report 83 Recommended Target Volume [39]..... 26

Figure 3. 1: Screenshot of Oncentra Masterplan Version 4.3 at Sweden Ghana Medical Centre. 36

Figure 3. 2: Gold markers (green) and field edge (red) annotations on the DRR and EPI. 38

Figure 4. 1: Scatter plot of displacements in vertical direction. 48

Figure 4. 2: Scatter plot of displacements in lateral direction. 49

Figure 4. 3: Scatter plot of displacements in longitudinal direction. 49

Figure 4. 4: The histogram of vertical displacement. 50

Figure 4. 5: The histogram of lateral displacement. 51

Figure 4. 6: The histogram of longitudinal displacement. 52

LIST OF ABBREVIATIONS

EBRT	External Beam Radiation Therapy
DNA	Deoxyribonucleic Acid
OARs	Organs at Risk
CTV	Clinical Target Volume
IM	Internal Margin
ITV	Internal Target Volume
SM	Setup Margin
PTV	Planning Target Volume
CT	Computed Tomography
ICRU	International Commission on Radiation Units and Measurement
GTV	Gross Tumour Volume
SD	Standard Deviation
RT	Radiotherapy
EPID	Electronic Portal Imaging Device
MLC	Multi-leaf Collimator
MU	Monitor Unit
MeV	Mega electron Volt
3DCRT	Three Dimensional Conformal Radiotherapy
LINAC	Linear Accelerator
3D	Three Dimensional
IMRT	Intensity Modulated Radiotherapy
IGRT	Image Guided Radiotherapy
VMAT	Volumetric Modulated Arc Therapy
KV	Kilo Voltage
POP	Parallel Opposed Pair
ROI	Region of Interest
MV	Mega Volt
DRRS	Digitally Reconstructed Radiographs

CHAPTER ONE

INTRODUCTION

1.1. Background

External beam radiation therapy (EBRT) in cancer treatment or management involves ionizing radiation delivered to a targeted point (the tumour) from an external source. The aim of EBRT is to deliver an optimum dose of radiation to cancer cells by destroying their deoxyribonucleic acid (DNA) while sparing the surrounding normal healthy tissues.

However, the journey from diagnosis to the radiation therapy treatment room requires planning and many steps involving many healthcare providers [1]. After a patient is diagnosed with cancer and the decision is made for radiotherapy, the patient has to undergo treatment simulation. During this process, the diseased area is imaged and localized for treatment planning procedure. However, there are some geometric uncertainties before and during treatment planning process and radiotherapy procedures.

Geometric uncertainty is a function of both the target volume and the organs at risk (OARs). A margin is therefore added to clinical target volume (CTV) to ensure that the target is adequately covered in all spheres. Internal organ movement is integrated by an internal margin (IM) around the CTV to make up the internal target volume (ITV). However, due to set-up errors, a setup margin (SM) is added to the ITV to yield the planning target volume (PTV).

When the patient is imaged to define the CTV and critical structures, the position is sampled. In general, this sample occurs once, specifically during the computed tomography (CT) scan for treatment planning [1]. To obtain this sample, the patient is immobilized and positioned, with typical reference marks placed on the skin and/or

immobilization device at the principal axes (isocentre) of the CT scanner for verification of position and orientation. The sample of the patient serves as the guide for treatment planning, and all subsequent targeting and density modelling is based on the information obtained during this session.

In 1993 and 1999, the International Commission on Radiation Units and Measurements (ICRU) issued report number 50 (ICRU-50) [3] and 62 (ICRU-62) [4] for prescribing, recording, and reporting photon beam therapy. The goal of these reports were to ensure standardization in specifying and reporting radiation doses in radiotherapy to provide important data for assessing the results of treatments. Thus, the ICRU 50 [3] and ICRU 62 [4] reports are regarded as worldwide standard for radiation therapy treatments. They establish guidelines to promote the use of a common language for specifying and reporting the doses in radiotherapy, as well as the volumes in which they are prescribed. However, EBRT treatment of prostate cancer involve several steps and procedures which inevitably introduces geometrical uncertainties. Several authors have presented data on set-up errors [11, 13] to calculate for error margins. With careful immobilization or well-designed setup protocols [14, 15], a setup for each axis of 2 mm standard deviation (SD) or better can be achieved for prostate cancer irradiation. The main source of these uncertainties includes:

a. tumour delineation inaccuracies of the gross tumour volume (GTV)
b. unknown extent of microscopic tumour
c. organ positional variation within the patient and
d. Set-up variations.

Recently, considerable efforts have been made by several authors [11, 13] to measure and reduce these geometrical errors. Nonetheless, residual errors always remain. In

conformal radiotherapy, these uncertainties are generally handled by adding a safety margin to the target.

Set-up errors are an intrinsic part of the radiation treatment process. They are defined as the difference between the actual and intended position with respect to radiation delivery. To account for accurate coverage of target volume depend on the set-up margins, which should be optimized to prevent unintended irradiation of surrounding normal tissues. Planning target volume that includes the clinical target volume with some margins to account for such uncertainties in patient positioning, organ motion, and beam geometry is universally accepted today as the standard for radiotherapy dose prescription [3, 4]. However, the use of portal imaging device to measure to localize tumour has become standard practice today. Hence, the use of EPID coupled with a demand to reduce PTV margins, particularly for high-precision radiotherapy has provided the drive for such assessments across the radiation oncology profession [8]. The experience, training, commitment and time available with radiation therapy staff can have a major impact on daily positioning accuracy. Therefore, the use of EPID is aimed at reducing human errors as low as possible.

However, it is generally recommended that every hospital establishes its own set-up accuracy without blindly adopting to publish margin recipes. It is for this reason that this study was carried out at the radiotherapy unit of Sweden Ghana Medical Centre (SGMC) to establish local departmental protocol PTV margin for prostate cancer patients.

Moreover, several margin formulae have been derived to account for CTV-PTV margins. Most commonly used margin recipe of Van Herk et al [10], Stroom et al [7] and ICRU 62 [4] published formulae were used to evaluate PTV margins in vertical, lateral and longitudinal directions for SGMC.

1.2. Statement of Problem

The rationale behind a successful radiotherapy is to give an accurate dose to a target volume whiles avoiding undue exposure of ionising radiation to the critical organs/healthy tissues.

Radiotherapy procedures introduces inevitable geometric uncertainties in treatment parameters. These uncertainties may emanate from:

- ✓ delineation of gross tumour volume (GTV)
- ✓ Unknown extent of microscopic tumour.
- ✓ Organ positional variation within the patient and
- ✓ Set-up variations.

To these extent, several authors such as van Herk et al [10], Stroom et al [7], ICRU report 62 [4] have deduced formulae that help determine setup margins. However, researchers have shown that these set-up errors vary from institutions/hospitals.

It is therefore prudent for every institution/hospital to determine their own CTV-PTV margin protocol.

Hence, this thesis established CTV-PTV margin during prostate cancer radiotherapy at SGMC.

1.3. Aims and Objectives

The primary objective of this study was to evaluate the set-up errors in prostate cancer radiotherapy and compare the results with international practices.

The specific objectives are; firstly, to calculate systematic and random errors in three major axes and secondly, to determined CTV-PTV margins using the published margin

formulae of ICRU 62, van Herk et al and Stroom et al in vertical, lateral and longitudinal direction of prostate cancer patients.

1.4. Relevance and Justification

Set-up errors are invariably accompanied by radiotherapy procedures. In other to account for adequate CTV- PTV margin, some margin recipes have been recommended to that effect. However, it is recommended that each institution/hospital determine their own CTV-PTV margin. This is to serve as protocol for radiation oncologists and medical physicists in determining CTV-PTV margin prior to treatment commencement.

1.5. Scope and Limitation

This work was carried out at Sweden Ghana Medical Centre.

The set-up errors in this thesis work were evaluated by generally accepted published formulae by the following authors;

ICRU report 62 [4], Marcel van Herk et al [10] and Stroom et al [7].

1.6 Organisation of the Thesis.

The organisation of this thesis/dissertation is as follow. Chapter one is an introduction to the research and provides an overview of the current state of knowledge relevant to the study. Chapter two is the reviews of existing literature relevant to the research problem. Chapter three focuses on the experimental and theoretical framework of the study. The results obtained were presented and discussed in chapter four. Chapter contains the conclusion of the study, recommendation and suggestion for further study.

CHAPTER TWO

LITERATURE REVIEW

2.0. Introduction

Radiation therapy has been the focus of penetrating research and development over the past few decades. Technological advancement have yielded substantial developments in treatment design, delivery and verification, mostly in the field of prostate cancer radiotherapy. The difficulty of prostate cancer radiotherapy has increased steadily as treatments have increasingly aimed to maximise tumour dose and minimise unwanted dose to normal tissue. However, introduction of IGRT (Image Guided Radiotherapy) have been at the centre of solving this increasing difficulties. The IGRT technology has therefore advanced from poor quality film, to electronic portal imaging for high-resolution of imaging of soft-tissue with the help of gold maker.

This thesis is to evaluate the set-up errors for prostate cancer treatment and establish CTV-PTV margin for prostate cancer patients using EPID at SGMC.

2.1. Prostate anatomy

Located deep within the male pelvis, the healthy prostate is found adjacent to the urinary bladder and rectum. The Figure 2.1 is schematic diagram of male pelvic anatomy. The prostate encircles part of the urethra. Thus, a narrow tube which carries urine out of the bladder to the penis. However, the proximity of the rectum and urinary bladder, as shown Figure 2.1, is highly to be considered during prostate cancer radiotherapy.

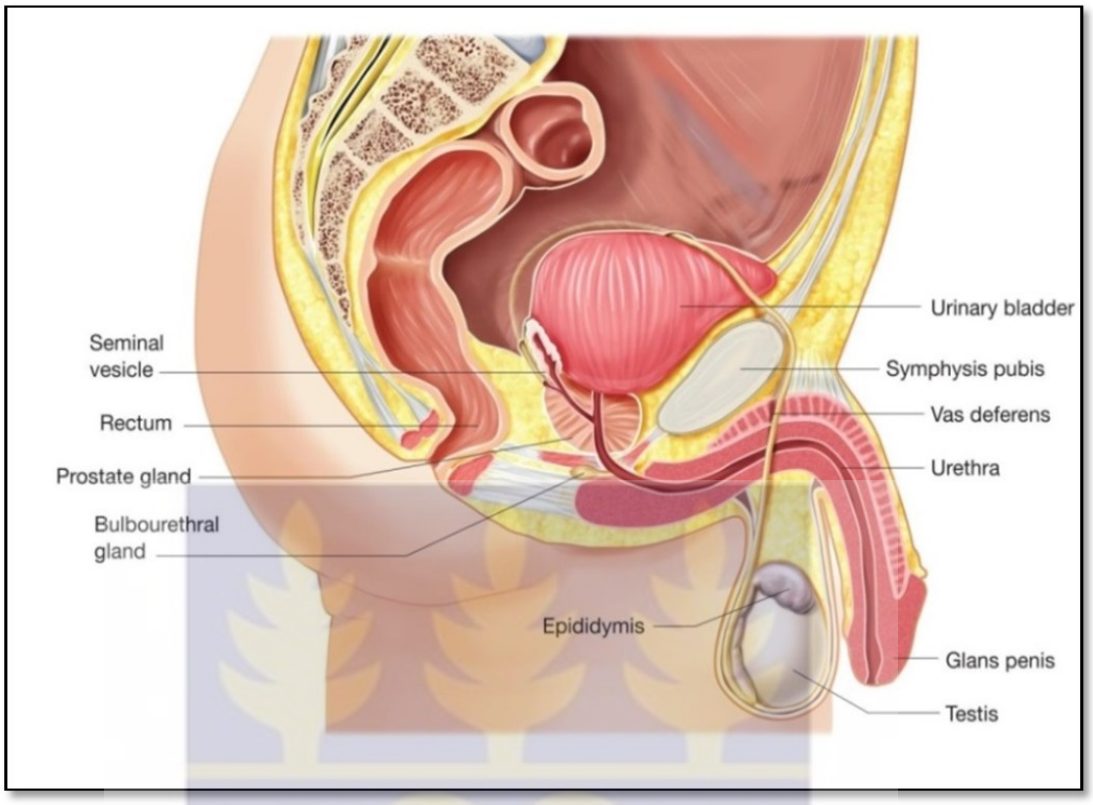

Figure 2.1: Sagittal view of male pelvic anatomy. From [42]

The Linear Accelerator

External photon beam radiation therapy is usually delivered using a linear accelerator, or linac, in which electrons are accelerated through interactions with a harmonised RF electromagnetic field. A magnet bending system directs the electron beam towards the patient in the case of electron treatments, or towards a target made of a material with a high atomic number in the case of photon irradiation. The electrons decelerate when they hit the target, and this energy loss is converted into bremsstrahlung photons [11]. The treatment head of the linear accelerator contains several components that scatter, filter, or shape the radiation beam. The schematic structure of the treatment head of an Elekta linear synergy 11 accelerator is shown in Figure. 2.2. Radiation fields from photon beams are shaped by a collimator system, where the main components are

primary and secondary collimators, wedges, and the multi-leaf collimator (MLC). A multi-leaf collimator consists of several pairs of “metal/leaves" placed in opposing leaf banks, where each leaf can move almost independently of the others.

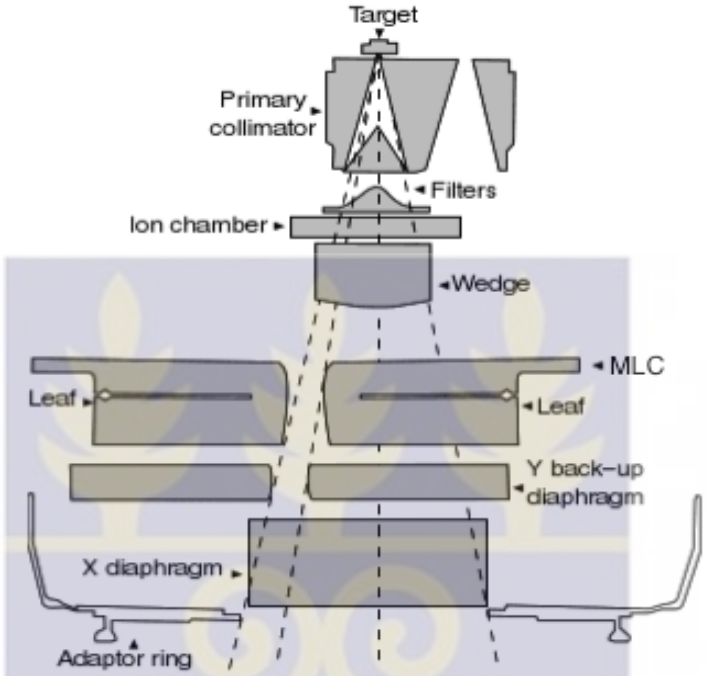

Figure 2. 2: A schematic diagram of an Elekta treatment head. Source [39]

The treatment head of linac is mounted on a gantry which is able to rotate 360° around the horizontal axis. The gantry angle is zero when the gantry is in the top position, i.e. directly above the patient with the radiation beam pointing vertically down, and the gantry angle increases as the gantry rotates clockwise. The collimator system can rotate 360° around the central axis of the photon beam. However, the treatment couch can move in vertical, lateral and longitudinal direction. Additionally, the couch can also rotate around the vertical axis.

The isocenter of the linac is defined as the cross section between the photon beam's central axis and the gantry's rotational axis [39]. During radiotherapy procedure, set of laser beams are used to mark the position of the isocenter. The laser beams helped in positioning the patient correctly before treatment.

The output from a linear accelerator is measured in monitor units (MU). The linear accelerators are usually calibrated to deliver 100 MU when an absorbed dose of 1 Gy is delivered to a point at a certain depth (10 cm for photons, the depth of maximum dose for electrons) in a water phantom. A clinical photon beam consists of a spectrum of energies, where the maximum energy equals the energy of the accelerated electrons, and the mean energy equals approximately 1/3 of the maximum energy [39].

2.2. Dosimetry

The intensity I(x) of a narrow monoenergetic photon beam that has been attenuated by passing through a material of thickness x is given by

$$I(x) = I(0)e^{-ux} \tag{2.1}$$

where I (O) is the original intensity of the unattenuated beam.

$\boldsymbol{u}$ is the linear attenuation coefficient, which depends both on the photon energy and the atomic number of the material. Multiple processes contribute to this attenuation, and the total linear attenuation coefficient can be given as the sum of atomic attenuation coefficients for these processes.

Transfer of photon energy to matter involve two-step process. In the first step, energy is transferred to secondary charged particles. Compton scattering is the predominating interaction through which energy is transferred from photons to charged particles in soft tissue (low atomic numbers) at energies used for radiotherapy. As shown in Figure 2.3, the atomic attenuation coefficient for

Compton scattering is proportional to the atomic number Z and decreases with energy [6].

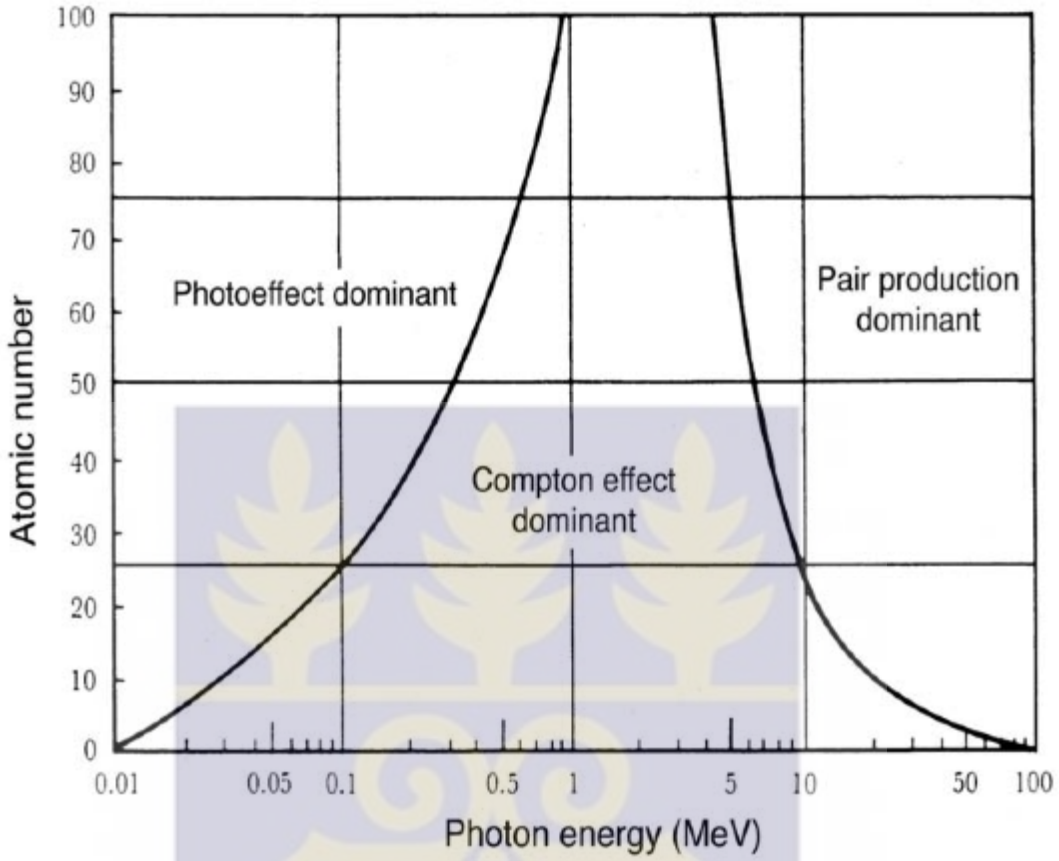

Figure 2. 3: Regions of relative predominance for the three main forms of photon interactions with matter for different atomic numbers Z and photon energies. From [41]

The secondary charged particles, later transfer some of their energy to matter via atomic excitations or ionizations.

The energy transferred in the first step of this process is known as KERMA (Kinetic energy released per mass unit). However, the second step results in absorbed dose D, which is defined as the mean energy dissipated by ionizing radiation per unit mass [6, 40]

2.2.1. Photon Fluence and Energy Fluence

Mono-energetic ionizing radiation beams are usually describe by the following quantities:

- Particle fluence
- Energy fluence
- Particle fluence rate
- Energy fluence rate

These quantities can be used to describe both photon beams and also charge particle beams.

2.2.2. Particle fluence ϕ

Particle fluence is very important basic quantity which describe the number of particles traversing a unit area in a certain point in space in a unit period of time. Assuming N particles passing through an area A, then particle fluence ϕ is the quotient of dN by dA, where dN is the number of particles incident on a sphere of cross-sectional area dA. i.e.

$$\phi = \frac{dN}{dA} \tag{2.2}$$

The unit of particle fluence is particles/cm^2 or particles/m^2. Particle fluence is independent of the incident angle of the radiation since the area considered for the sphere of cross-sectional is perpendicular to the direction of each particle. On the hand, planar particle fluence is the number of particles crossing a plane per unit area and hence depends on the angle of incidence of the particle beam.

2.2.3. Energy Fluence (ψ)

The descriptive quantity that takes into account the energies of the individual rays is the energy fluence ψ, for which the energies of all the rays are summed up. Therefore, energy fluence ψ can be define as the quotient of dR by dA, where dR is the radiant energy incident on a sphere of cross-sectional area dA. That is:

$$\psi = \frac{dR}{dA} \tag{2.3}$$

The unit of energy fluence is J/m^2 or $ergcm^{-2}$.

2.2.4. Particle Fluence Rate ($\dot{\phi}$)

The particle fluence rate $\dot{\phi}$, is the quotient of $d\phi$ by dt where $d\phi$ is the increment of the fluence in the time interval dt:

$$\dot{\phi} = \frac{d\phi}{dt} \tag{2.4}$$

The units of particle fluence rate is particles. $M^{-2}.s^{-1}$.

2.2.5. Energy fluence Rate $\dot{\psi}$

The energy fluence rate $\dot{\psi}$ (also referred to as intensity) is the quotient of $d\psi$ by dt, where $d\psi$ is the increment of the energy fluence in the time interval dt:

$$\dot{\psi} = \frac{d\psi}{dt} \tag{2.5}$$

The unit of energy fluence rate is W/m^2 or $J{\cdot}m^{-2}\ s^{-1}$.

2.2.6. Exposure X

Exposure is the quantity most common used to express the amount of radiation delivered to a point. Exposure X can be define as the quotient of dQ by dm, where dQ is the absolute value of the total charge of the ions of one sign produced in air when all the electrons and positrons liberated or created by photons in mass dm of air are completely stopped in air. I.e.

$$X = \frac{dQ}{dm} \tag{2.6}$$

The orthodox unit for exposure is the Roentgen R. In the SI system of units, roentgen is no longer used. Hence, the unit of exposure is simply 2.58×10^{-4} C/kg of air.

The convention of Roentgen to C/kg:

$$1\ R = 2.58*10^{-4}\ C/kg \tag{2.7}$$

$$1\ C/kg = 3876\ R \tag{2.8}$$

2.2.7. Exposure Rate $\dot{X}$

The exposure rate $\dot{X}$, is the quotient of $d\dot{X}$ by dt, where $d\dot{X}$ is the increment of exposure in the time interval dt, thus:

$$\dot{X} = \frac{dX}{dt} \tag{2.9}.$$

The unit of exposure rate is $Ckg^{-1}s^{-1}$.

2.2.8. Absorbed Dose (D)

The energy of ionizing radiation are readily deposited in human tissue upon interaction with the human body. The amount of energy deposited depend on the penetrating ability of the radiation, the size and the density of body section. However, some of the human tissue or organs are more susceptible to ionizing radiation than others. As a non-stochastic quantity, absorbed dose is applicable to both indirectly and directly ionizing radiations. For indirectly ionizing radiations, energy is imparted to matter in a two-phase process. Thus, step the first phase (resulting in Kerma) where indirectly ionizing radiation transfers its energy as kinetic energy to secondary charged particles. And also, the second phase involve charged particles transferring some of their kinetic energy to the medium (resulting in absorbed dose) and loses some of their energy in the form of bremsstrahlung losses. The absorbed dose is related to the stochastic quantity energy imparted at a specific point within the body tissue. Therefore, absorbed dose can be defined as the mean energy $\bar{\varepsilon}$ imparted by ionizing radiation to matter of mass m in a finite volume V by:

$$D = \frac{d\bar{\varepsilon}}{dm} \tag{2.10}$$

The energy imparted ε is the sum of all energy entering the volume of interest minus all energy leaving the volume, taking into account any mass-energy conversion within the volume. Pair production, for example, decreases the energy by 1.022 MeV, while electron-positron annihilation increases the energy by the same amount. Also, because the electrons travel in the medium and deposit energy along their tracks, this absorption of energy does not take place at the same location as the transfer of energy described

by Kerma. The unit of absorbed dose is joule per kilogram ($J \cdot kg^{-1}$). The special name for the unit of absorbed dose is the Gray (Gy).

2.2.9. Integral Dose

The integral dose is the total amount of energy absorbed in the body. The integral dose account for the total mass of tissue exposed. The conventional unit for integral dose is the gram-rad, which is equivalent to 100 ergs of absorbed energy. The idea behind the use of this unit is that, if all absorbed doses (rads) are added for each gram of tissue in the body, it will have been an indication of total absorbed energy. Since the integral dose is quantity of energy with SI unit of joule. The relationship between Joule and gram-rams is given as:

$$1\ J = 1000\ \text{gram-rads} \tag{2.11}$$

Integral dose is probably the radiation quantity that most closely correlates with potential radiation damage during diagnostic procedure. Integral dose does not reflects only the concentration of radiation absorbed in the tissue but also the amount of tissue affected by the radiation.

2.2.10. Kerma (K)

Kerma is an acronym for Kinetic Energy Released per unit Mass. It is a non-stochastic quantity which is applicable to indirectly ionizing radiations, such as photons and neutrons. It quantifies the average amount of energy transferred in a small volume from the indirectly ionizing radiation to directly ionizing radiation and ionization. Usually, dissipation of photon energy to matter involve two main stages. For the first stage, the photon radiation transfers energy to the secondary charged particles (electrons) through

various photon interactions (photo-effect, Compton Effect, pair production, etc). In the second stage, the charged particle transfers energy to the medium through atomic excitations and ionisations. For that matter, Kerma can be defined in this context as the mean energy transferred from the indirectly ionizing radiation to charged particles (electrons) in the medium $d\bar{E}_{tr}$ per unit mass dm:

Mathematically,

$$K = \frac{d\bar{E}_{tr}}{dm} \tag{2.12}$$

The unit of Kerma is joule per kilogram ($J \cdot kg^{-1}$). The special name for the unit of Kerma is the gray (Gy), where

$$1\ Gy = 1\ J \cdot kg^{-1} \tag{2.13}$$

2.2.11. Cema (C)

Cema is the acronym for Converted Energy per unit Mass. It is a non-stochastic quantity use to directly describe ionizing radiations, such as electrons and protons. The Cema C is the quotient of dEc by dm, where dEc is the energy lost by charged particles, except secondary electrons, in electronic collisions in a mass dm of a material:

$$C = \frac{dE_c}{dm} \tag{2.14}$$

The different between Cema and Kerma is that Cema involves the energy lost in electronic collisions by incidence charged particles. However, on the other hand, Kerma involves the energy imparted to the traversing charged particles.

The unit of Cema is joule per kilogram ($J \cdot kg^{-1}$). The special name for the unit of Cema is the Gray (Gy).

2.2.12. Organ Dose

Both external and internal radiation could result into organ dose (i.e. exposure radiation to organ). Measurement/calculation of organ dose from external radiation is usually more straightforward than for internal radiation. Following an intake of radioactive material, there is a time period during which the material gives rise to equivalent doses delivered in organs or tissues of the body at varying rate. The time integral of equivalent-dose rate is called the committed equivalent dose, $H_{T\,(\tau)}$, where τ is the irradiated time.

2.2.13. Equivalent Dose (H_T)

Equivalent Dose (H_T) in a tissue T is a quantity mostly use to indicate the biological impact of radiation on persons receiving occupational, environmental exposure. Personnel exposure in a clinical facility is often determined and recorded as equivalent dose.

The equivalent dose in tissue T is given as:

$$H_T = \sum W_R D_{T,R} \qquad (2.15)$$

where $D_{T,R}$ is the absorbed dose average over the tissue or organ T, due to radiation R and W_R is a weighting factor called radiation weighting factor selected for a particular type and energy of the radiation incident on the body. The radiation weighting factor, W_R, represents the relative biological effectiveness of the incident radiation in producing stochastic effects at low doses in tissue or organ T. Most radiation encountered in diagnostic and therapeutic procedures (X-ray, gamma, and beta) has quality and modifying factor values of 1. Hence, the absorbed dose is numerically equal to equivalent dose. Some other types of radiation have quality factor greater than 1. Example include, alpha particles, which have quality factor of approximately 20**.** The unit of equivalent dose is the joule per kilogram with special name of Sievert (Sv).

2.2.14. Effective Dose

The radiation exposure of the organs and tissues of the human body results in different probabilities of detriment for the different organs and for different individuals. For radiation protection purposes, the ICRP has introduced the effective dose, E, as a measure of the combined detriment from stochastic effects for all organs and tissues for an average adult. It is the sum over all the organs and tissues of the body of the product of the equivalent dose, H_T, to the organ or tissue and a tissue weighting factor, W_T, for that organ or tissue:

$$E=\sum W_T H_T \tag{2.16}$$

But the tissue weighting factor, W_T, for organ or tissue T represents the relative contribution of that organ or tissue to the total detriment arising from stochastic effects

for uniform irradiation of the whole body. The sum over all the organs and tissues of the body of the tissue weighting factors, W_T, is unity.

The SI unit for effective dose is the Sievert (Sv).

2.3. Techniques in Radiotherapy

Technological advancement in radiotherapy instrumentation has receive massive improvement in the past decade. Hence, accurate localization and treatment of disease has become possible. The invention of the Multileaf Collimator (MLC) has revolutionized conventional field shaping permitting the fast and easy production of complex and irregular field shapes [31]. An MLC is collimation system in the treatment head consisting of several narrow tungsten leaves. Each MLC leaf is motorized and individually controlled allowing the treatment beam fields to be shaped around the target itself. MLCs can contain from 60-120 leaf pairs. The widths of MLC can range from 1mm to 1cm depending on the linac design [6].

2.3.1. Three Dimensional Conformal Radiation Therapy

The invention of multi-leaf collimation in treatment planning gave rise to one of the most common treatment planning techniques used today. I.e. Three Dimensional Conformal Radiation Therapy (3DCRT). Before 3DCRT came into the light, treatment field shapes were limited to just squares and rectangles fields. With this modality, the dose distributions were box shaped and high dose are given to the target volume. However, with the introduction of the MLC into the treatment head, high dose regions are now able to be shaped to conform to the target [32]. Here, computed tomography (CT) data acquired in the simulation is used to conform the high dose region to the target in all three planes, hence the term “Three Dimensional Conformal Radiation

Therapy". The 3DCRT technique reduces the volume of normal tissue exposed to radiation as compare to the two dimensional conventional radiotherapy treatment techniques [31]. This has seen tremendous reduction of radiation to healthy tissues during treatment.

2.3.2. Intensity Modulated Radiation Therapy

Intensity Modulated Radiotherapy differs from 3DCRT by modulating the photon fluency of the linear accelerator (LINAC) during treatment as opposed to keeping it constant which occurs in conventional treatments. Thus, IMRT employs radiation beams with non-uniform intensities to produce dose distributions more conformal than 3DCRT techniques [31]. I.e. it uses 3-D scans of the patient body to guide the beams of radiation to the tumour from many different angles. However, in IMRT, inverse treatment planning method is use contrary to conventional forward planning. Inverse treatment planning requires that the medical physicists (the treatment planner) to put in the goals of the treatment in terms of the desired dose to the target and surrounding organs into a treatment planning program. Using an optimization engine, the treatment planning program then finds the optimal radiation beam intensity distributions which satisfy the user specified goals [16].

2.3.3. On Board Imaging and IGRT

The On-Board Imager acquires high-quality digital images in the treatment room, allowing for positioning of patient accurately before treatment. The On-Board Imager consists of a kV X-ray source and an amorphous silicon panel that can be added to the Linac configuration.

The On-Board Imager employs robotically controlled arms that operate with three axes of motion, optimizing positioning of the imaging system for the best possible view of the target.

The On-Board Imager makes Dynamic Targeting (IGRT) more efficient and convenient. This device detects movement due to changes in patient setup, internal organ movement or movement associated with breathing.

It enables users to:

• Improve tumour targeting, thus improving the effectiveness of treatments,

• Reduce side effects by reducing treatment margins,

• Develop new treatments using hypofractionated techniques.

2.3.4. Volumetric Modulated Arc Therapy (VMAT)

A further development of IMRT is volumetric modulated arc therapy (VMAT), with which radiation is delivered as the gantry rotates around the patient. There is a continuous modulation of the rotation speed of the gantry, the MLC field shape and the delivered dose rate [26, 38]. The treatment is given as one or more arcs, where each arc can cover up to 360° and move either clockwise or anticlockwise.

The term dual arc denotes the delivery of two oppositely oriented arcs covering the same gantry angles, where the optimization seeks to minimize the leaf travel.

2.4. Dosimetric Characteristics of Radiation Beam

Radiation beams are characterized by the type of radiation as well the energy of the radiation. The linac design and the medium through which the radiation passes also influences the radiation beam.

However, radiation beams produced by an individual linac need to be characterized to enable accurate beam modelling (e.g. flatness, quality) for dose calculation [1]. Usually, due to tissue equivalent property of water and it's universally availability, most radiation beams are characterized in water phantom.

The main concern about characterizations of a clinical radiation beam is the amount of dose that are deposited along the longitudinal axis of the beam. This is defined as the central axis depth dose curve which is a graphical representation of the dose variation as a function of depth in tissue, measured along the central axis of the beam [16]. Central axis depth dose curves provide relevant information such as:

- ✓ the surface or skin dose,
- ✓ the depth in tissue where the maximum dose point occurs (d_{max})
- ✓ as well as the rate of dose falloff as a function of depth along the central axis.

The dose indicates the percentage of the maximum dose. Central axis depth dose curves enable's one to characterize the build-up region of a radiation beam. That is the area between the skin and d_{max}. Figure 2.4a shows several central axis depth dose curves representing beams of different energies. Hence, as beam energy increases, the depth of d_{max} increases, the skin dose decreases, also the rate of dose falloff decreases.

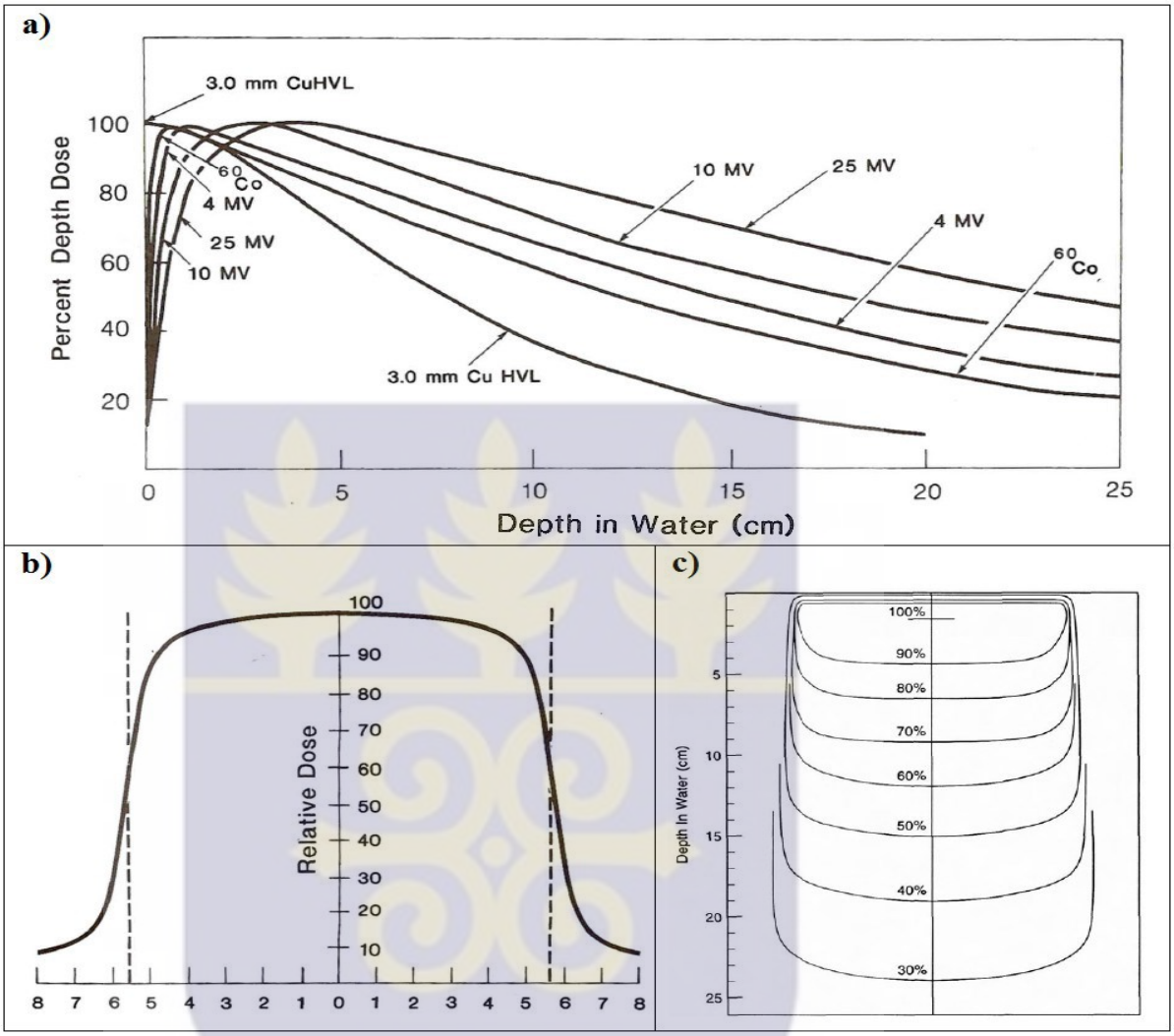

Figure 2. 4: a) Central axis depth dose curves of multiple beam energies [16]. (b) Typical Co-60 beam profile. c) Typical 6MV isodose chart [17]. (a) and (b) taken from Khan [16], (c) taken from Karzmark et al [17].

2.4.1. Radiation Beam Combination

The classification of a single radiation beam is very vital for clinically accurate dose calculation in treatment planning. For most radical treatment plans, a combination of two or more beams is used to concentrate the high dose to the target volume. This volume is usually located centrally within the patient. However, the distribution of dose for multiple beams can be attained by adding linearly the overlapping isodose charts of

the individual beams. The dose for treatment plans with multiple beams is most often normalized to 100% dose level that occurs at the isocentre. Moreover, the dose at all other points within the distribution are relative to the isodose. The most common multi-beam arrangement is usually termed parallel opposed pair (POP). This involves two identical beams positioned 180^0 from one another, providing a more uniform dose distribution at the centre of the patient. A parallel opposed pair dose distribution has a characteristic shape with the maximum dose occurring at the entrance and exit point of the beams and the minimum dose occurring in the centre as shown in figure. 2.4.

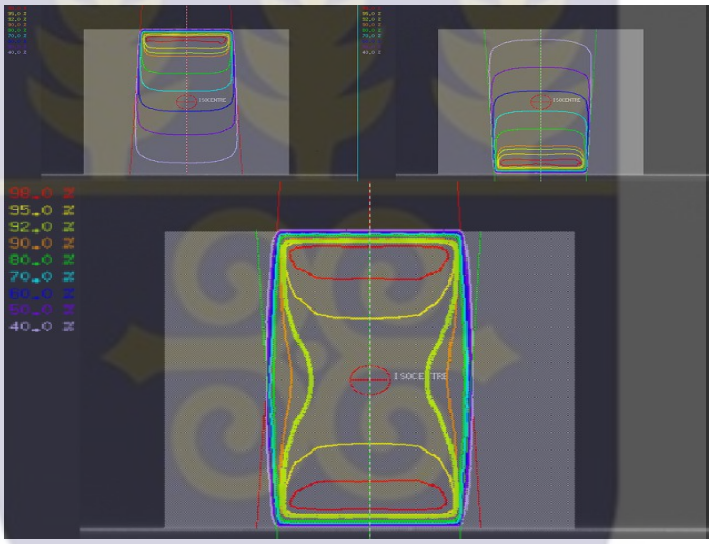

Figure 2. 5: Combination of posterior and anterior fields to produce parallel opposed dose distribution [1].

Moreover, when two parallel opposed beams are positioned orthogonally to each other, the high dose region at the centre of the patient forms a box shape creating a common beam configuration known as four field box (Figure 2.5). This shape can also be achieved with three beams; however the high dose "box" will be located closer to the surface of the patient along the central axis of the unopposed beam. The shape of the high dose area can be modified by altering the number of beams, their angles and the amount of radiation delivered by each beam relative to one another (termed beam weighting). The optimal beam configuration for a treatment plan is dependent on the

treatment site, the required shape of the high dose area and the presence of surrounding sensitive organs.

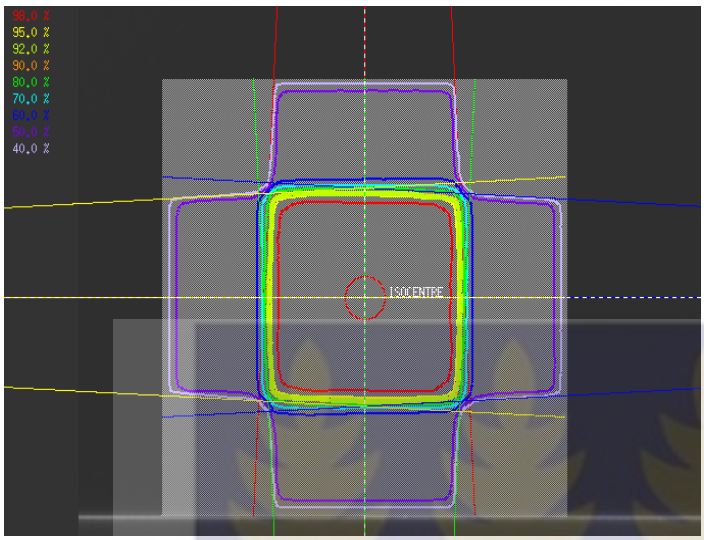

Figure 2. 6: Dose distribution for four field box technique [1]

2.5. Volume Delineation

The design of a treatment plan begins with the identification and delineation of certain regions of interest (ROIs) in the patient's images. These ROIs can be divided into target and risk volumes. A precise definition of these volumes is essential for plan design and evaluation, treatment documentation and follow up. The Figure. 2.6 shows the variation in PTV volume delineation of a teacher, students and groups.

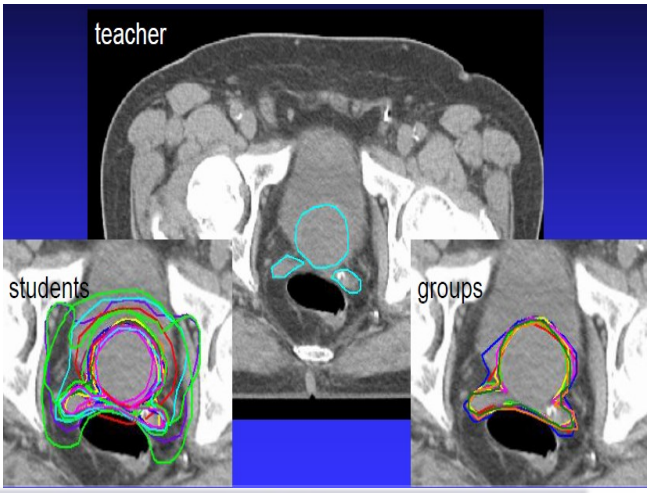

Figure 2. 7: Delineation of PTV by the teacher, students and the groups at ESTRO teaching course.

The volumes and margins mentioned here are defined in guidelines from the ICRU [17, 18].

2.5.1. Target Volumes

The target volumes recommended in ICRU Report 83 [17, 18] are listed below and illustrated in Figure. 2.6.

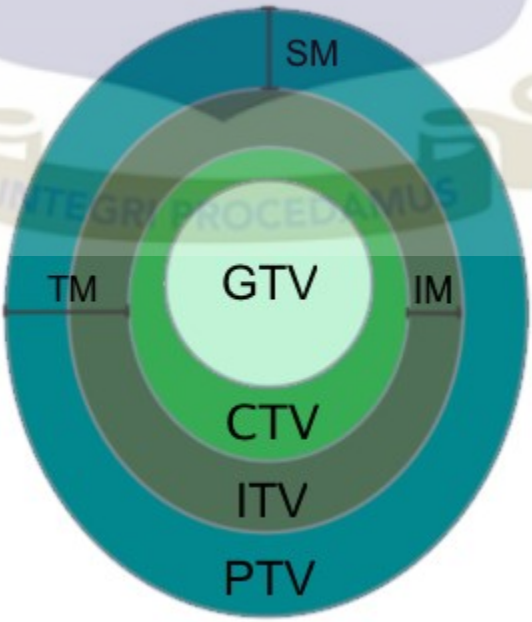

Figure 2. 8: ICRU Report 83 Recommended Target Volume [39].

- The gross tumour volume (GTV) is the palpable or visible extent of malignant growth.
- The clinical target volume (CTV) contains a GTV and/or areas where there is probability of malignant growth is high.
- The internal target volume (ITV) is generated by adding an internal margin to the CTV.
- The planning target volume (PTV) is generated by adding a setup margin to the ITV.

  This margin accounts for uncertainties in patient positioning, equipment uncertainties, image-transfer errors, dosimetric uncertainties, and other factors from fraction to fraction. When an ITV is not defined, the PTV is expanded directly from the CTV. In this case, a total margin combining the internal and setup margin is added.

These margins can be uniform over the whole volume or vary in different directions. GTV and CTV are anatomical volumes in the patient, while ITV and PTV are geometrical volumes, independent of the patient geometry.

2.5.2. Organs at Risk

All healthy tissue is at risk of damage when exposed to radiation. During treatment planning, certain normal tissues classified as organs at risk (OARs) are delineated. In prostate cancer patients, the rectum and the bladder are considered as organs at risk (OARs). These are normal tissues whose radiation sensitivity may influence the treatment planning and/or the dose prescription. Limitations are set on the dose to these organs.

2.6. Organ Movement

Internal organ movement inherently introduces geometric uncertainty in set-up errors. Most studies done on organ movement have been prostate movement, as well as breathing-induced movement in the thorax and abdomen. Langen et al have published an excellent review of the magnitude of organ movement as studied by several investigators [18]. Prostate movement is due to pelvic setup variation and internal movement of the prostate within the pelvis. However, primary factors that affect prostate movement are rectal and bladder filling, with variance influence of these forces in prone against the supine patients. In other to reduce geometric uncertainty, most of the prostate patients are positioned supine. This is to give the patient comfort as well as to improve in setup variation of the prostate. Predominantly, prostate movement studies have been done on interfractional position changes. But some measurements have been made on intrafractional movement. However, breathing has been shown to impact prostate movement, most notably during deep breathing and in prone patients [29, 30]. Peristalsis, gas in the rectum, and bladder filling have a more significant influence on prostate position and potentially short-term movement [16]. Current research has shown that implanted electromagnetic markers (gold markers) has help to track the position of the prostate in between treatment fractions. Prostate movement can be reduced by diet and immobilization through a rectal balloon. Mostly, the attempts that are made in managing prostate movement was to focus on localization. Radiographic localization and tracking of implanted markers, has become routine practice.

2.7. Derivation of systematic and random set-up errors and relationship to the CTV- PTV margin.

The random and systematic set-up errors for a group of patients may be derived from electronic portal images.

2.7.1. Set-up error

The set-up error (Δ) is defined as the deviation between actual and intended position during radiotherapy procedure. This is calculated as a shift in the isocentric position when an image is compared against its corresponding reference. The EPID is usually placed in orthogonal direction with the treatment head of the linac (for example, A–P and S–I from a lateral image and R–L and S–I from an anterior image). However, if the acquired images are not in orthogonal direction, it must be converted into the appropriate co-ordinate axes. Vector quantities are also calculated so that correct direction information is maintained. For example, if shifts in the anterior direction are given a negative sign then those in the posterior direction are always positive.

$$m_{indiv} = \frac{\Delta_1+\Delta_2+\Delta_3+\cdots+\Delta_n}{n} \qquad (2.15)$$

where $\Delta_1, \Delta_2, \Delta_3 \ldots\ldots \Delta_n$ are the individual set –up errors/shifts on the vertical, lateral and longitudinal direction and n is the average number of fraction per patients.

2.7.2. Total population mean set-up error

The total mean set-up error (M_{pop}) is all mean for the analysed patient group and should ideally be zero. Significant departures from zero indicate an underlying error common to this patient group and requires investigation. Hence, this parameter is a strong indicator of the effectiveness of any given treatment technique and is usually neglected. The equation is individual patient (m_1, m_2, m_3 …) mean being summed up and the total divided by the number of patients in the group (P).

$$M_{pop} = \frac{m_1+m_2+m_3+....+m_p}{P} \qquad (2.16).$$

2.7.3. Population systematic error

The systematic error for the population ($\sum_{set\text{-}up}$) is defined as the SD (spread) of the individual mean set-up errors about the overall population mean (M_{pop}). Thus, systematic error is calculated as:

$$\sum = \frac{(m_1-M_{pop})^2+(m_2-M_{pop})^2+(m_3-M_{pop})^2+\cdots+(m_n-M_{pop})^2}{(P-1)} \qquad (2.17)$$

2.7.4. Random set-up errors

The random component of any error is a deviation that can vary in direction and magnitude for each delivered treatment fraction [42].

When considering geometric uncertainties in radiotherapy, the term ‘random error’ consist of individual patient or the treatment population.

2.7.5. Individual Random Error

It is calculated by summing the squares of the differences between the mean and set-up error from each image in turn. I.e. the individual random error is given as:

$$(\sigma_{individual})^2 = \frac{(\Delta_1 - m)^2 + (\Delta_2 - m)^2 + (\Delta_3 - m)^2 + \cdots + (\Delta_n - m)^2}{(n-1)} \quad (2.18)$$

where m is the mean, Δ is the set-up error for each image.

2.8.5 Population Random Error

The population random error (σ) is the mean of all the individual random errors (σ_1, σ_2, σ_3 ….σ_p). This equation assumes that the number of images acquired per patient is identical or that any differences will have minimal effect on the final result. Hence, the population random error is calculated as:

$$\sigma = \frac{\sigma_1 + \sigma_2 + \sigma_3 + \cdots + \sigma_p}{p} \quad (2.19)$$

where P is the total patient population

2.8. Margin derivation

Several population-based margin calculation recipes have been proposed. These recipes are combination of systematic and random errors. Systematic occurs during treat preparation whiles the random errors occurs during treatment execution time.

These margin calculation recipes can be expressed as:

$$\mathrm{CTV-PTV margin} = a\sum + b\sigma + c \qquad (2.20)$$

where $\sum$ and σ are the combined sum of the standard deviations of all contributing systematic and random errors respectively and a, b and c are constants. McKenzie AL et al [43] has included a constant c to account for parameters that affect the margin in a linear manner.

However, the two constants a and b characterise the relative contributions of the systematic and random components and these depend on factors such as the beam arrangement and chosen coverage probability [44]. In calculating the CTV-PTV margin, several formulae has been recommended. In this study, the margin formulae considered are ICRU Report 62, van Herk and Stroom published margin recipes.

The margin recipe recommended by ICRU is given as:

$$\mathrm{CTV-PTV\ margin} = \sqrt{(\sum^2 + \sigma^2)} \qquad (2.21)$$

Stroom's CTV-PTV margin formula is given as:

$$\mathrm{CTV\ to\ PTV\ margin} = 2\sum + 0.7\sigma \qquad (2.22)$$

Due to geometric errors for the prostate. Their formula is defined as follows;

$$2.5\sum + 0.7\sigma - 3\ \mathrm{mm} \qquad (2.23)$$

Where $\sum$ and σ have their usual meaning as described in equation (4.1)

CHAPTER THREE

MATERIALS AND METHODS

3.0. Introduction

The materials and methodologies adopted to evaluate the three-dimensional set-up errors in vertical, lateral and longitudinal axes are outlined in this chapter. In this study, the planning target volume (PTV) were determined using the well-recognized margin formulae. The formulae employed in this study include; the ICRU 62 [4], van Herk et al [10] and Stroom et al [7] margin formula.

3.1. Materials

3.1.1. Linear Accelerator

At Sweden Ghana Medical Centre, the linear accelerator (LINAC) manufactured by Elekta Synergy 11 was used for the radiotherapy procedure. The LINAC has dual energy photon beam of 6 and 15 MV and electron beam of 6, 10 and 15 MV. The electrons are produced by an electron accelerator and accelerated to their desired speed through an accelerating waveguide and interact with a target material of high atomic number to produce the treatment beam. The beams are made up of Bremsstrahlung x-ray spectrum and are characterized by nominal accelerating potential [5]

With the help of Multileaf Collimator (MLC), the treatment beams are collimated, filtered and monitored within the treatment head of the LINAC in order to produce a clinically useful radiation beam which delivers a uniform dose distribution at a specified depth in water. The machine output is measured in monitor units (MU) in which individual machines are calibrated to deliver a specific absorbed dose per MU

(usually 1Gy/MU). Plate 3.1 below is the linac used for treating cancer patients in Sweden Ghana Medical Centre.

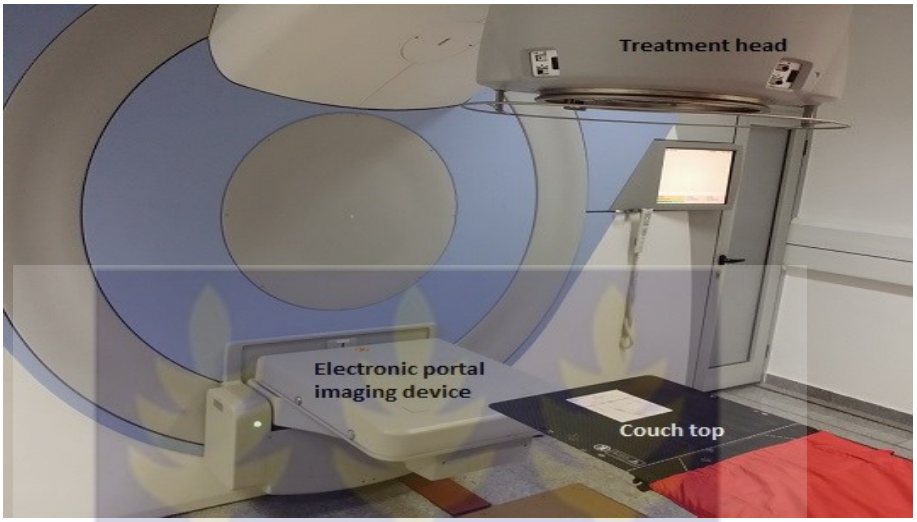

Plate 3. 1: State –of- art Linear Accelerator at Sweden Ghana Medical centre.

3.1.2. The iViewGT™ Electronic Portal Imaging Device

A typical configuration of the iViewGT™ portal imaging device includes an amorphous silicon (a-Si) flat mega voltage (MV) panel image detection system with powerful image processing and display. The EPID deliver superior image quality and collection of analysis tools that improve clinical decision-making [33]. The EPID aid in the reduction of treatment setup errors and the quality assurance and verification of complex treatments. EPIDs are used to track the position of the tumour in real time. However, at Sweden Ghana Medical Centre, EPID which was mounted isocentrically on the Linear Accelerator (LINAC) with a detector size of 30×30 cm; aids in tracking the tumour location during radiotherapy procedure. Acquisition of images are fully automated and are comprehensively analysed to present GUI the in single monitor at the control room. The images were taken when X-rays passes through the patient and activate a fluorescent screen and the amorphous silicon panel that captures the resultant

light. The dose range of iViewGT is 2 to 4 MUs. It monitors its own dose system to ensure optimum dose from the fluorescent screen and amorphous silicon panel is used to acquire the portal image [43]. Gold markers are typically inserted into the prostate using trans-rectal ultrasound guidance. The markers aid in tracking the displacement of the tumour per each treatment fraction daily.

3.1.3. Treatment Planning System

The enhanced collapsed cone (CC) convolution algorithm (Oncentra Masterplan Collapse Cone Version 4.3) TPS was used as treatment planning platform for CT image importing, contouring and 3DCRT treatment planning. A screenshot from an Oncentra Masterplan Version 4.3 planning graphical user interface (GUI) is shown in Figure 3.1. It offers a variety of advanced tools for treatment planning, optimization, CT image registration, automatic contouring (autocontouring) for delineating tumour and organs at risk. The Oncentra Masterplan has planning tools such as dose calculation as well as positioning the treatment beams and isocentre.

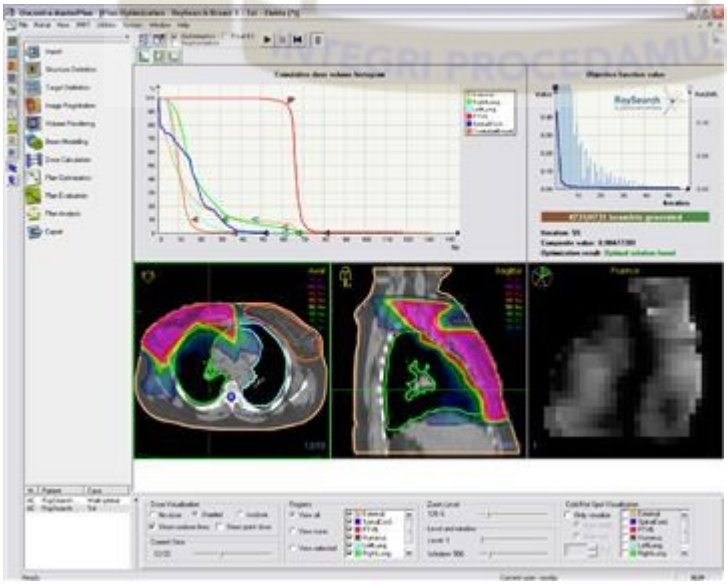

Figure 3. 1: Screenshot of Oncentra Masterplan Version 4.3 at Sweden Ghana Medical Centre.

3.2. Methods

3.2.1. Data Selection

Localized Prostate cancer patients who underwent high dose (max of 78Gy/39fractions) 3DCRT were used for this research. Three gold markers were inserted into their prostate as a surrogate to track the movement of the prostate on daily bases. The EPID with the iViewGT software was used to determine the online displacement before treatments. Those displacements are recorded for all the fractions and analysed using the margin formulae to establish the departmental CTV-PTV margin.

The data consists of prostate cancer patients treated with 3DCRT from May, 2012 to June, 2016. However, patients who received an average of 30 fractions of radiotherapy with vertical, lateral and longitudinal directions portals images were analysed. Also patients with at least 3 sets of orthogonal portal images were included in the dataset. In all, a total of 54 patient's data were analysed.

3.2.2. Immobilization and Simulation using the CT 16 slice.

Each patient was inserted with three fine cylindrical gold markers (1 × 8 mm) trans-rectally into the prostate; using ultrasound guidance by an urologist before treatment planning. Patients were scanned supine, with their hips immobilized from the waist to mid-thigh in a rigid foam cradle and with the lower legs supported in a soft foam immobilization device. Planning CT images were taken at 3 mm slice thickness from the top of the first lumbar vertebrae to below the pelvis. Patients were asked to empty their bowels (taking 10 mg of dulcolax) 2 days prior to scanning, and their bladder was

kept comfortably full by drinking two glasses of water mixed with 18 mls of gastrografin 30 minutes prior to scanning. Magnetic resonance imaging (MRI) scans were also taken and fused with that of the CT scans for treatment Planning. The prescribed dose to the isocentre was 78 Gy in 39 fractions over 7.8 weeks.

3.2.3. Portal Imaging and Analysis

Portal images were acquired using iViewGT™ Portal Imaging Device made of amorphous Silicon base detector. The EPID system is a camera-based consisting of a detector screen, light enclosure, optical chain, camera and video capture [34]. It is mounted isocentrically on the linear accelerator with a detector size of 30 cmx30 cm. It acquired images at a reduced dose of 2-4 MUs per field for portal acquisition. These images were compared to the corresponding DRRs.

Systematic errors in prostate displacement were calculated as the average of the individual means of the measured prostate displacements for each patient. After aligning of the marker positions onto the reference images as shown in Figure 3.2, the set-up deviations corrections are shown and an on-line correction procedure are effected. Lateral (+ sign for left shift and – sign for right shift), longitudinal (+ sign for superior and – sign for inferior shift) and vertical shifts (+ sign for anterior shift and – sign for posterior shift) are done manually to correct these random and systematic errors before the actual treatment doses are administered. Random errors were calculated as the average trend for errors to occur about each mean displacement errors.

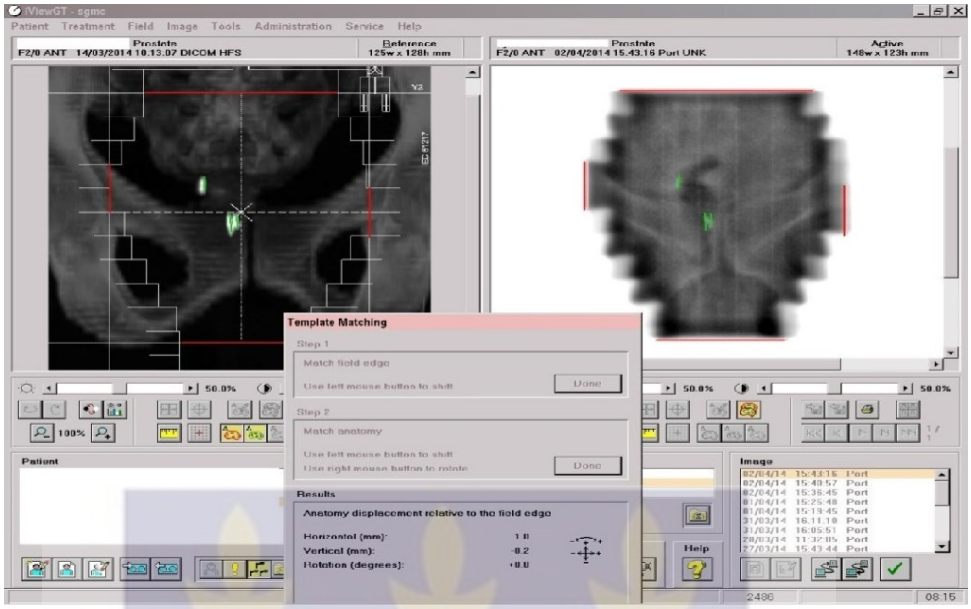

Figure 3. 2: Gold markers (green) and field edge (red) annotations on the DRR and EPI.

3.2.4 Radiation Treatment Technique

Before each treatment fraction, the first 4 and 2 monitor units (MUs) of the lateral and anterior treatment fields were used to take portal images. The gold markers from the DRRs were also manually matched unto the images. A shift threshold of 3 mm was used for the prostate migration corrections and any translations of more than that were corrected before each treatment. The setup error is estimated and the patient position is corrected to reduce the discrepancies between the localization and reference images. The anterior treatment fields are used to locate the lateral and longitudinal prostate motion whiles the lateral treatment fields, are used for the vertical prostate motion. After the corrections are done through repositioning of the patients, a verification image is taken to confirm the shift before the actual treatment is given.

3.3. Set-up Errors

The set-up errors in vertical, lateral and longitudinal direction can be analysed theoretically from the portal images acquired. Systematic errors can be broadly regarded as treatment preparation errors that affects all fractions. It can cause the effect of shifting the overall dose distribution. Random errors are those broadly regarded as treatment execution errors, affecting each fraction individually.

3.3.1. Population Systematic Error

The population systematic error were determined using the formula:

$$(\sum_{set-up})^2 = \frac{(m_1 - M_{pop})^2 + (m_2 - M_{pop})^2 + (m_3 - M_{pop})^2 + \cdots + (m_n - M_{pop})^2}{(P-1)} \quad (3.1)$$

where $m_1, m_2, m_3, \ldots\ldots m_n$ are the individual mean, P is the total patient population in the group and M_{POP} is the overall mean for the total population given as:

$$M_{pop} = \frac{m_1 + m_2 + m_3 + \ldots + m_p}{P} \quad (3.2)$$

3.3.2. Population Random Errors

The total random errors were also calculated in vertical, lateral and longitudinal directions.

The population random error is thus given as;

$$\sigma_{set-up} = \frac{\sigma_1+\sigma_2+\sigma_3+\cdots+\sigma_p}{p} \quad (3.3)$$

where σ_1, σ_2, σ_3, …….σ_p are the individual random errors and P is the total population of the patients.

3.4. PTV Margin calculation

The CTV-PTV margins were calculated using the International

Commission on Radiation Units and Measurements (ICRU) Report 62 [4], Stroom's [7, 28], and van Herk's [10, 36] published formulae.

Table 3.1 below illustrate the published formulae use by above mention authors.

Table 3. 1: Published CTV-PTV Margin Formulae.

	CTV-PTV margin formulae
ICRU Report 62	$\sqrt{(\sum^2+\sigma^2)}$
Van Herk	$2.5\sum+0.7\ \sigma$-3 mm
Stroom	$2\sum+0.7\ \sigma$

CHAPTER FOUR

RESULTS AND DISCUSSIONS

Results

4.0. Introduction

This chapter presents the results and discussion thereof obtained from displacement analysis of prostate cancer patients during radiotherapy procedure at Sweden Ghana Medical Centre (SGMC).

The Table 4.1 below shows the individual patient mean, overall mean and the systematic errors in vertical, lateral and longitudinal direction.

Table 4. 1: Table of individual means, overall mean and systematic error in three directions.

		Orthogonal directions (mm)		
Pat. #	Mean Errors	Vert.	Lat.	Long.
1	m_1	-1.9867	-0.9567	-2.5344
2	m_2	-3.6033	-0.6667	-1.5933
3	m_3	0.86	-0.29	0.8333
4	m_4	0.4733	2.8533	-3.3333
5	m_5	0.0433	-1.8333	-5.1567
6	m_6	-2.9133	-3.06	-4.4733
7	m_7	-0.1933	2.41	-0.6733
8	m_8	-0.7467	1	-0.69
9	m_9	-1.6233	0.1833	-1.3333

10	m_{10}	-1.2933	0.4533	-4.11
11	m_{11}	-1.23	-2.7867	-2.9033
12	m_{12}	-0.0067	-1.6402	0.6241
13	m_{13}	0.4467	0.1167	2.2367
14	m_{14}	1.6867	-0.3467	0.6067
15	m_{15}	-0.2467	1.2172	-1.22
16	m_{16}	0.82	-3.3633	0.2733
17	m_{17}	0.5367	0.6233	-2.9367
18	m_{18}	1.0167	8.29	2.6533
19	m_{19}	0.3034	-0.9233	-1.9333
20	m_{20}	-1.03	1.69	3.1967
21	m_{21}	-1.18	1.3433	1.66
22	m_{22}	-1.5867	0.8633	1.2233
23	m_{23}	-1.0033	0.0867	0.59
24	m_{24}	-1.1933	-0.7933	1.8
25	m_{25}	-5.3967	1.4033	-3.8733
26	m_{26}	-0.6767	0.31	-2.979
27	m_{27}	2.6067	-0.5	-2.9467
28	m_{28}	3.84	1.3867	-2.9467
29	m_{29}	2.4767	0.78	0.2433
30	m_{30}	-2.0567	0.9333	0.3133
31	m_{31}	-1.3667	2.35	-2.0633
32	m_{32}	1.84	-0.6367	1.3167
33	m_{33}	1.7067	5.0533	0.3733
34	m_{34}	-0.2767	0.2433	-0.6367

35	m_{35}	-2.6333	2.86	-0.57
36	m_{36}	-2.3133	2.3367	-2.8167
37	m_{37}	-0.0967	-6.6833	2.6567
38	m_{38}	-1.4533	3.96	-2.2933
39	m_{39}	0.2733	-1.8067	0.3067
40	m_{40}	0.9567	-1.8633	2.8433
41	m_{41}	-1.15	-10.7733	2.75
42	m_{42}	0.0367	-3.09	1.7167
43	m_{43}	-6.59	1.48	-4.9067
44	m_{44}	-0.9033	-3.2633	2.96
45	m_{45}	0.4467	4.18	2.6733
46	m_{46}	1.39	-0.4933	0.7967
47	m_{47}	0.02	1.47	0.7933
48	m_{48}	-0.6067	0.5133	-0.6267
49	m_{49}	-1.3367	-1.2833	0.15
50	m_{50}	-0.6767	-1.49	-6.4967
51	m_{51}	1.0567	-1.2533	1.7367
52	m_{52}	-1.75	-1.7433	-0.3433
53	m_{53}	0.5933	3.0374	3.09
54	m_{54}	-0.9933	0.7167	4.1867
Overall population mean(mm)	M_{pop}	-0.49413	0.04823	-0.40344
Population Systematic Set-up Errors(mm)$\sum$		1.807554	2.826408	2.505365

Table 4. 2: Individual patient's random errors and overall mean of random errors.

Random Errors				
	3-D Orthogonal directions (mm)			
Pat. #	Random Errors	Vert.	Lat.	Long.
1	σ_1	2.547	4.131	2.6409
2	σ_2	3.0988	3.9958	2.1231
3	σ_3	2.2152	4.2454	3.2355
4	σ_4	3.3772	3.055	3.165
5	σ_5	5.4923	5.4475	3.4947
6	σ_6	2.9891	3.3807	5.7476
7	σ_7	2.6736	2.0889	3.0283
8	σ_8	2.4236	1.4496	2.0099
9	σ_9	2.4425	2.9608	2.7768
10	σ_{10}	3.4505	1.9602	5.7849
11	σ_{11}	2.4563	3.5105	2.3114
12	σ_{12}	2.9849	3.8342	2.316
13	σ_{13}	3.5807	3.3243	2.356
14	σ_{14}	3.0189	3.1014	2.1233
15	σ_{15}	2.832	1.368	1.8054
16	σ_{16}	2.1376	4.6304	1.7231
17	σ_{17}	6.7514	5.0466	2.7634
18	σ_{18}	3.2171	8.5133	3.4572
19	σ_{19}	2.1195	3.5843	4.4121

21	σ_{20}	1.4935	3.9274	7.4374
20	σ_{21}	2.9663	3.6115	2.3768
21	σ_{22}	2.1757	3.078	1.7791
23	σ_{23}	2.2415	1.7865	2.5311
24	σ_{24}	3.2575	3.9903	3.8376
25	σ_{25}	5.7937	4.8826	5.752
26	σ_{26}	4.5095	3.0733	3.1716
27	σ_{27}	3.2346	3.7322	5.0871
28	σ_{28}	2.8681	1.815	5.0871
29	σ_{29}	2.9986	2.6195	3.8292
30	σ_{30}	3.2235	3.1909	1.7156
31	σ_{31}	3.9505	4.2068	5.1854
32	σ_{32}	4.0612	4.3133	3.1763
33	σ_{33}	3.206	6.3999	4.8597
34	σ_{34}	2.051	4.445	2.6458
35	σ_{35}	4.4097	3.3177	6.8174
36	σ_{36}	2.8555	4.036	5.2129
37	σ_{37}	2.5848	7.9485	6.7486
38	σ_{38}	4.6045	6.3023	5.3481
39	σ_{39}	3.3502	4.4017	4.093
40	σ_{40}	3.1834	4.8079	1.9732
41	σ_{41}	3.099	5.7714	5.2891
42	σ_{42}	5.9149	8.0101	4.5041
43	σ_{43}	3.9226	5.6613	4.3985
44	σ_{44}	2.6953	5.2101	6.364

45	σ_{45}	3.52	7.8553	4.9423
46	σ_{46}	2.652	4.9064	3.3365
47	σ_{47}	2.446	2.4262	2.7803
48	σ_{48}	2.1176	2.4992	3.5366
49	σ_{49}	2.8121	4.3728	5.8499
50	σ_{50}	3.0449	4.4998	9.5651
51	σ_{51}	3.9001	6.8857	2.7901
52	σ_{52}	2.4081	4.2088	3.221
53	σ_{53}	2.3232	3.0374	1.9843
54	σ_{54}	2.7858	2.1667	2.3738
Population Random Set-up Errors σ (mm)		3.193872	4.1301	3.831022

The total population mean, systematic and random errors were shown in table 4.3

Table 4. 3: The values of overall means, random errors and systematic errors.

	3-D Orthogonal Directions (mm)		
	Vertical	Lateral	Longitudinal
Overall Mean			
M_{POP}	-0.49	0.05	-0.40
Random Error			
$\sigma_{set\text{-}up}$ (mm)	3.19	4.13	3.83
Systematic Error			
$\sum_{set\text{-}up}$ (mm)	1.81	2.83	2.51

Table 4.4 below contains the calculated CTV-PTV margin using ICRU 62(1999), Stroom et al (2002) and Van Herk et al (2000) margin recipes.

Table 4. 4: PTV margin in vertical, lateral and longitudinal direction

	CTV-PTV margin for prostate cancer (mm)		
Direction	ICRU 62 $\sqrt{(\sum^2+\sigma^2)}$	Stroom $(2\sum+0.7\sigma)$	van Herk $(2.5\sum+0.7\sigma-3$ mm)
Vertical	3.67	5.85	3.75
Lateral	5.00	8.54	6.96
Longitudinal	4.58	7.69	5.95

The Figures 4.1-4.3 were the scatter plots of displacements in vertical, lateral and longitudinal direction.

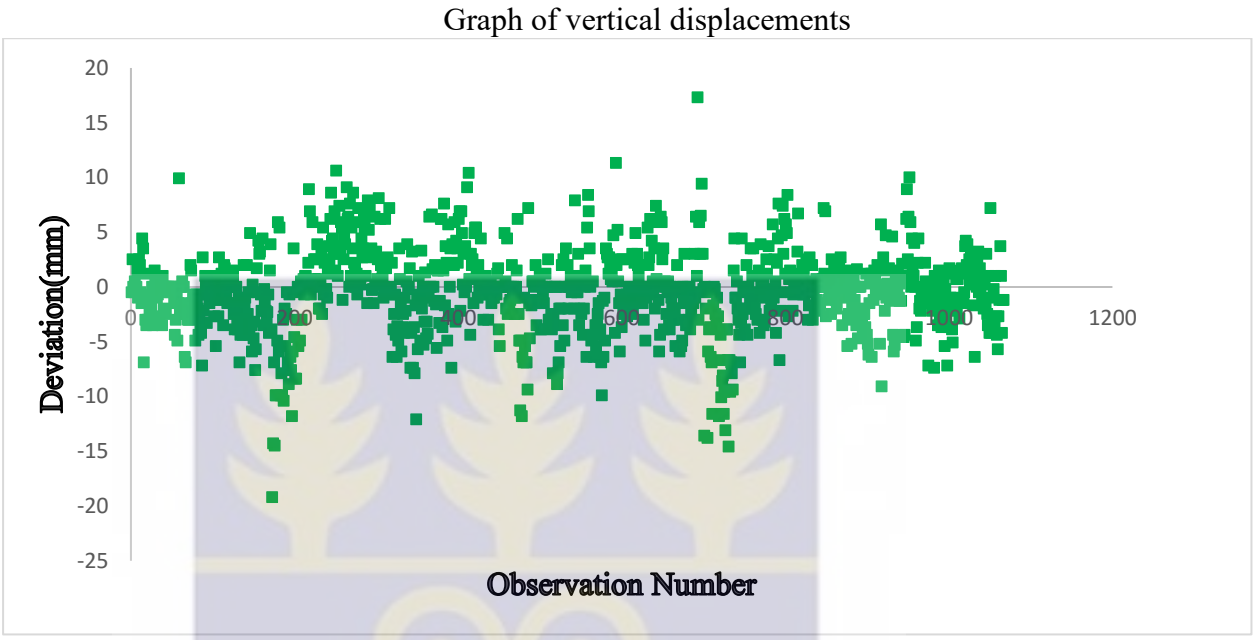

Figure 4. 1: Scatter plot of displacements in vertical direction.

Graph of lateral displacement

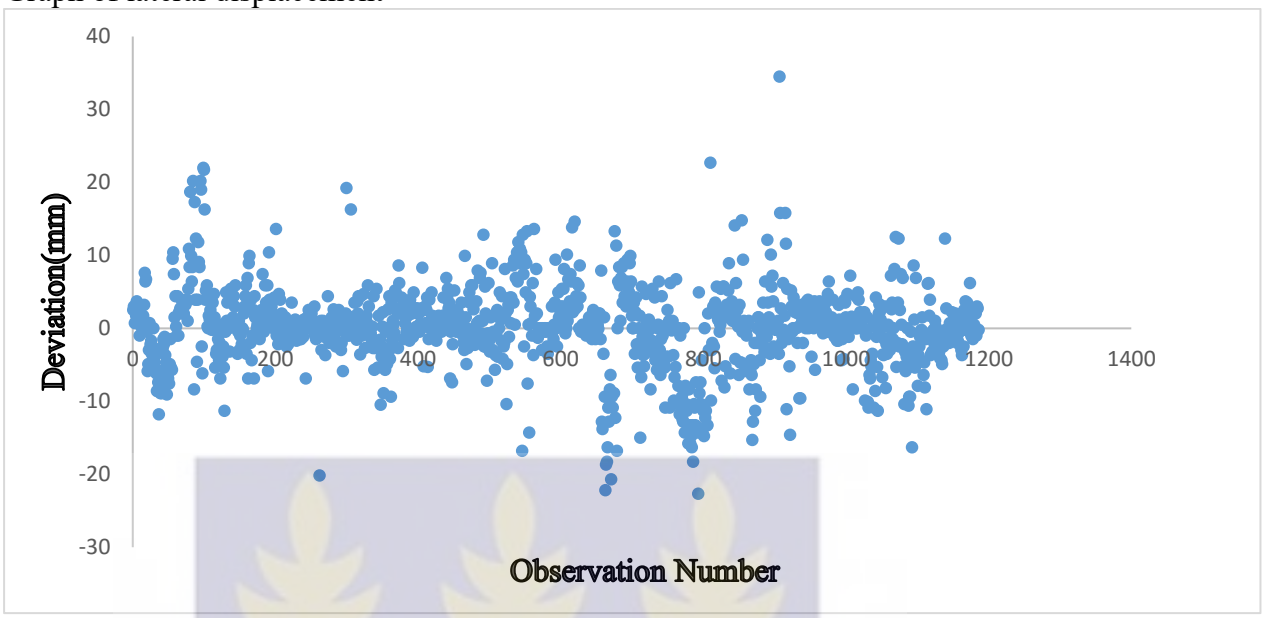

Figure 4. 2: Scatter plot of displacements in lateral direction.

Graph of longitudinal displacements

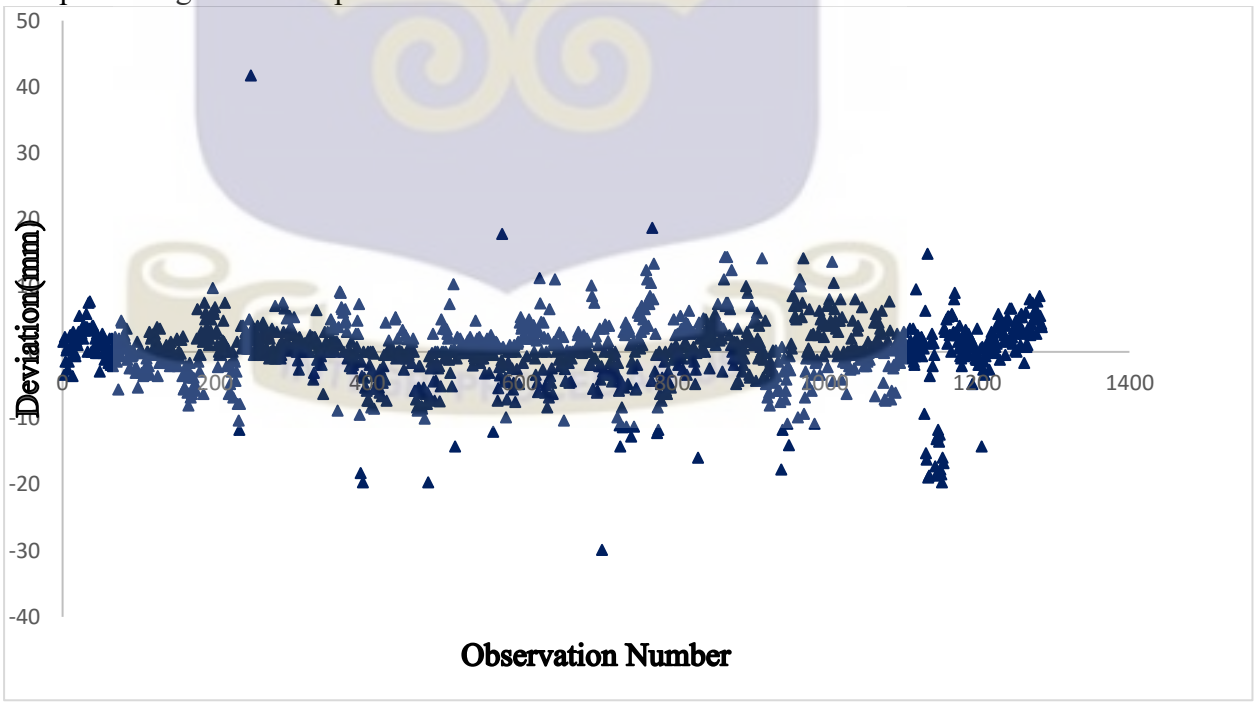

Figure 4. 3: Scatter plot of displacements in longitudinal direction.

Figures 4.4-4.6 were the histograms of translational displacements in vertical, lateral and longitudinal direction.

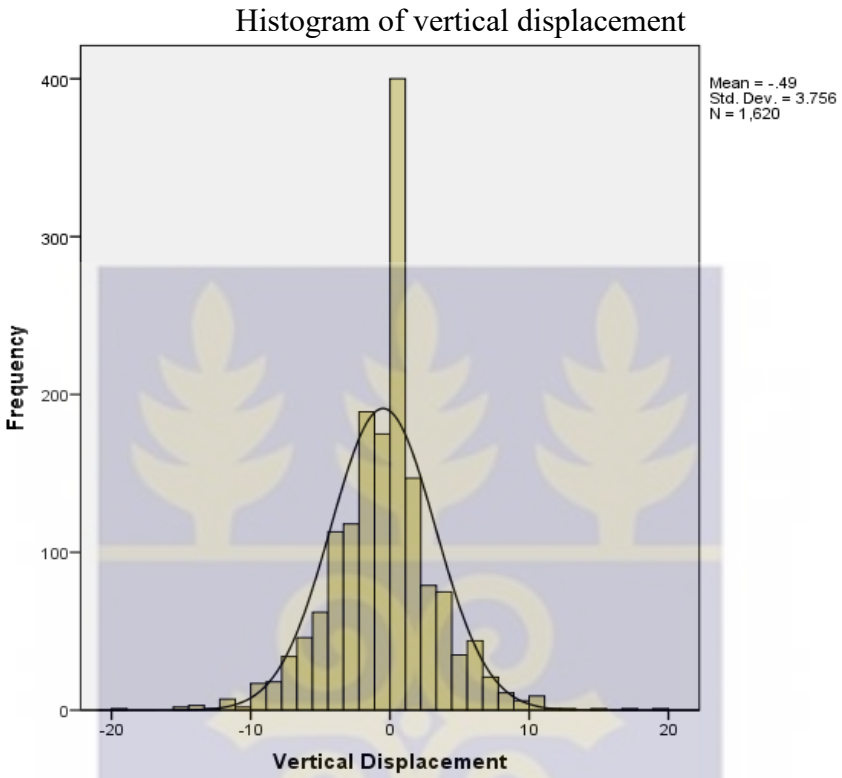

Figure 4. 4: The histogram of vertical displacement.

Lateral displacement

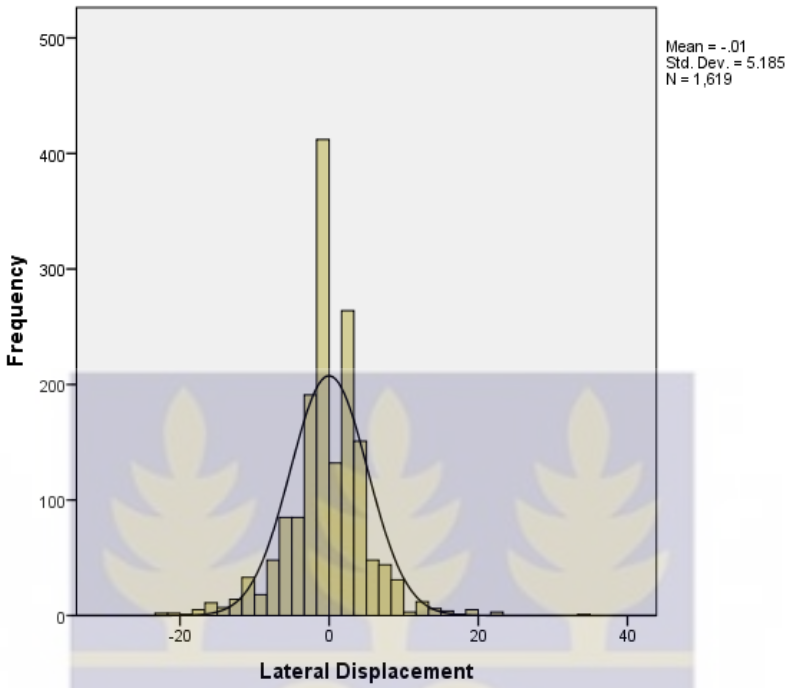

Figure 4. 5: The histogram of lateral displacement.

Histogram of longitudinal displacements

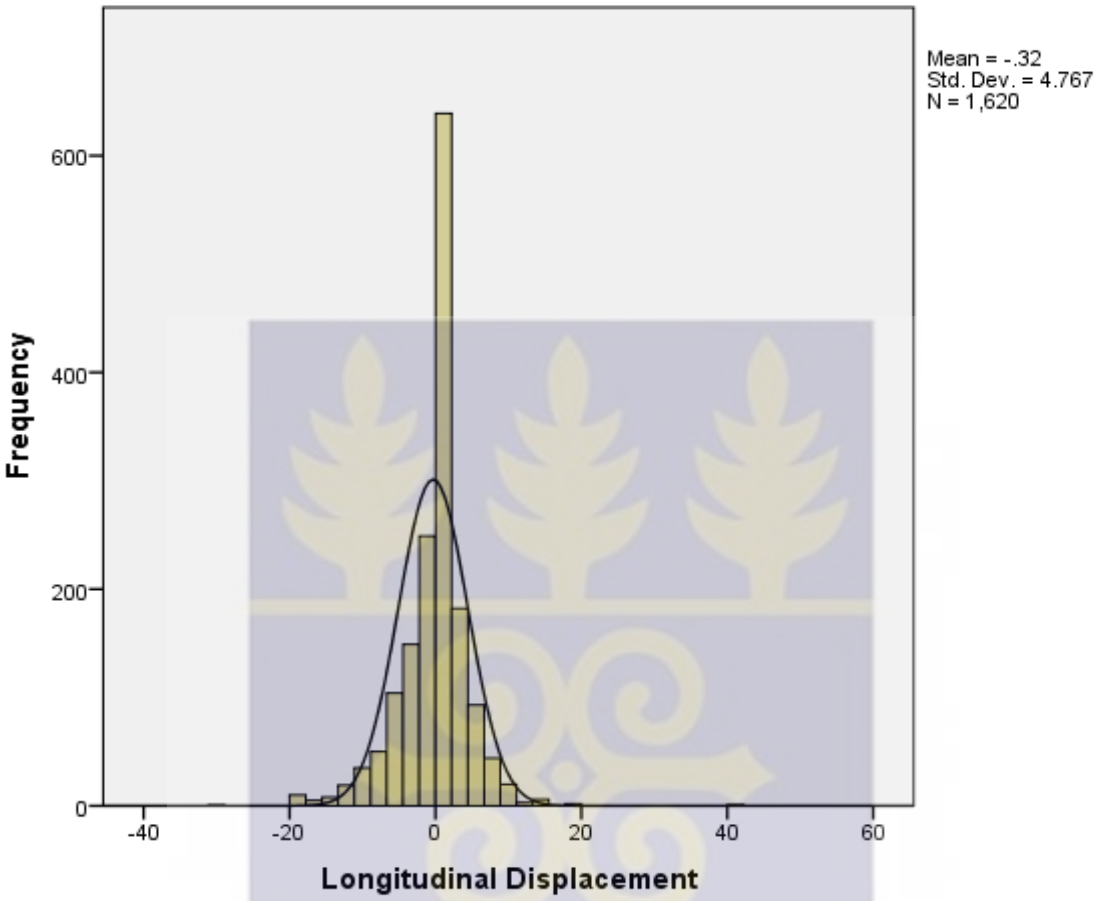

Figure 4. 6: The histogram of longitudinal displacement.

Discussions

4.1. Overview

The values of three dimensional displacements of prostate cancer cases were evaluated in vertical, lateral and longitudinal direction in this study. A total of fifty-four prostate cancer patients' set-up error data were analysed. The statistical tools used for the analysis were the Statistical Package for Social Sciences, StatPlus 2009 Professional 5.8.0, and Microsoft office Excel (2013) were used to analyse the data. The

displacements/shifts in prostate cancer patients along vertical, lateral and longitudinal direction were presented in Appendix A.

4.2. Individual Mean and Total Population Mean.

The mean for individual patients in the three directions were calculated by finding the average of set-up errors. Table 4.1 shows the individual patients mean in vertical, lateral and longitudinal directions. However, the overall mean for vertical, lateral and longitudinal direction were also calculated by taking the average of individual mean. Hence, -0.49 mm, 0.05 mm and -0.40 mm were the overall mean for vertical, lateral and longitudinal direction respectively and the standard deviation in vertical, lateral and longitudinal axes were 3.75 mm, 5.20 mm and 4.76 mm respectively.

4.2.1. Population Systematic (∑) and Random (σ) Errors

Systematic (Σ) and random (σ) errors were calculated using statistical software SPSS, StatPlus 2009 Professional, and Microsoft excel (2013). The systematic component of the displacement characterizes the displacement that was present during the entire course of treatment. For an individual patient, the mean represent systematic component of all the displacements. Moreover, for the whole population the systematic error was represented by the standard deviation (SD) from the values of mean displacement for all individual patients. However, random errors represent routine discrepancy in the set-up of the patient. For the total patient population, the distribution of random error displacements was expressed by the root mean square of SD of all patients. Hence, the population systematic error (Σ) along vertical; lateral; and longitudinal direction were 1.81 mm, 2.83 mm and 2.51 mm respectively as shown in Table 4.3. On the other hand, the population random error (σ) in the corresponding vertical, lateral and longitudinal

directions were 3.19 mm, 4.13 mm and 3.83 mm respectively. Population systematic errors (Σ) and random errors (σ) also correlated well with the published literature. According to ICRU 62 [4], the population systematic and random errors should be within <5 mm.

4.2.2. CTV-PTV Margin Calculation.

The CTV-PTV margins were calculated using the International Commission on Radiation Units and Measurements (ICRU) Report 62 [4], Stroom et al [28], and van Herk et al [10]. These margin formulae were illustrated in Table 4.4.

Based on International Commission on Radiation Units and Measurement (ICRU) recommendation, the CTV-PTV margin with respect to vertical; lateral; and longitudinal direction were 3.67 mm, 5.00 mm and 4.58 mm respectively. Secondly, the corresponding values of vertical, lateral and longitudinal direction using Stroom's formula were 5.85 mm, 8.54 mm and 7.69 mm accordingly.

Thirdly, the CTV-PTV margin in vertical, lateral and longitudinal direction using van Herk's margin recipe were 3.75 mm, 6.96 mm and 5.96 mm respectively.

4.2.3. Scatter Plots in the three Displacements

Scatter plots of displacements for all observations in all three directions were given in Figures 4.1-4.3. These scatter plots in vertical lateral and longitudinal direction were achieved using Microsoft Excel office (2013). They indicate that the set-up errors were normally distributed.

4.2.4. Histogram in the three Directions

According to central limit theorem, the distribution of the sum of an increasing number of errors with arbitrary distribution will approach normal (Gaussian) distribution. Figures 4.4-4.6, shows Gaussian distributions for the set-up errors in all the three (X, Y, Z) directions.

Significant shifts were observed in the vertical, lateral and longitudinal displacement for the prostate cancer patients. However, the use of EPID has enabled localization of target in prostate cancer, hence all the displacements in the vertical, lateral and longitudinal directions were within the published literature of <5 mm [4].

There are several mathematical recipes that have been recommended by many authors for calculating CTV-PTV margins. In ICRU report 62, the assumption is that both random and systematic errors have an equal effect on dose distribution. However, this may not necessarily be true. Random errors blur the dose distribution whereas systematic errors cause a shift of the cumulative dose distribution relative to the target [42]. Using coverage possibility matrices and dose-population histograms, Stroom et al. [28], van Herk et al. [36] have suggested formulae which incorporate this differential effect. Electronic portal imaging device (EPID) is a useful tool for a fast and reliable assessment and correction of various geometrical errors during the whole process of radiotherapy.

In modern image-guided radiation therapy (IGRT) systems, online tracking of variation in target positioning at the time of the treatment can be achieved. Hence, an accurate and adequate dose to the target can be obtained. IGRT is a good technique which help to localize and conform dose distribution within the tumour.

CHAPTER FIVE

CONCLUSIONS AND RECOMMENDATIONS

5.1. Conclusions

The general aim of this study was to evaluate three dimensional set-up errors (i.e. systematic and random errors) in vertical, lateral and longitudinal direction of prostate cancer patients who have received 3DCRT. Specific aim was to use the set-up errors to calculate the CTV-PTV margin for prostate cancer patients.

It was observed that, there are significant differences in displacements for the vertical, lateral and longitudinal directions considered in this study. However, the overall mean displacements obtained in all the three directions were within the published literature of <5 mm.

Among calculated CTV-PTV margins according to three published formulae (Table 4.3), the calculated margins there were differences in all the three displacements; which confirmed to those obtained by Thasanthan et al [2] on pelvic radiotherapy. ICRU Report 62 [4] has recommended optimum margins for target volume coverage to be within <5 mm in all three directions. Using ICRU Report 62 [4] margin formula, the CTV-PTV margin for vertical, lateral and longitudinal were 3.67 mm, 5.00 mm and 4.58 mm respectively. Moreover, van Herk PTV margin were 3.75 mm, 6.96 mm and 5.96 mm for vertical, lateral and longitudinal displacement respectively. Lastly, using Stroom PTV margin recipe; obtained CTV-PTV values were 5.85 mm, 8.54 mm and 7.69 mm in vertical, lateral and longitudinal displacement accordingly. The results confirmed that the dose escalation technique for treating prostate cancer patients are safe since none of the PTV margins calculated exceeded the conventional addition of 10 mm to CTV margin to obtain PTV margin. However, comparing the calculated PTV

margins, the values obtained by Stroom margin formula were recommended for maximum PTV coverage.

In conclusion, the use of gold markers and electronic portal imaging device for daily verification of position and correction of patient setup and prostate displacement has helped in establishing the appropriate PTV margin in prostate cancer radiotherapy.

5.2. Recommendations.

The following are the recommendations made to the professionals in 3DCRT of prostate cancer patients at SMC.

5.2.1. Medical Physicists

From this study, it was observed that there were significant differences in the three major vertical, lateral and longitudinal displacements. Therefore, to manage random and systematic errors effectively it was suggested that set-up errors need to be evaluated weekly to update departmental local PTV margin.

5.2.2 Oncologists

It is recommended that a new departmental local PTV margin must be establish in prescribing CTV-PTV margin prior to treatment commencement.

5.2.3. Further Study

There was also the need to evaluate CTV-PTV margin for other types of cancers. Example, head and neck, breast cancer, cervical cancer etc.

REFERENCES

[1]. Ecclestone Gillian, (2012). Assessing the Clinical Application of the Van Herk Margin Formula for Lung Radiotherapy.

[2]. Thasanthan L, Piyasena WRO, Croos AMC, Dhanushia R and Narayanan PP, (2014). Assessment of Three-Dimensional Set-up Errors in Pelvic Radiation Therapy.

[3]. International Commission on Radiation Units and Measurements (ICRU), (1993). Prescribing, recording and reporting photon beam therapy. ICRU-50, (ICRU, Bethesda, MD).

[4]. International Commission on Radiation Units and Measurements (ICRU), (1999). Prescribing, recording and reporting photon beam therapy (Supplement to ICRU Report 50) ICRU-62, (ICRU, Bethesda, MD).

[5]. Karzmark C.J, Nunan C.S and Tanabe E., (1993). Medical electron accelerators, (McGraw-Hill, Inc, Health Professions Division).

[6]. Podgorsak E.B, (2005). Radiation oncology physics: a handbook for teachers and students. (International Atomic Energy Agency, Vienna).

[7]. Stroom JC, de Boer HC, Huizenga H, Visser AG (1999). Inclusion of geometrical uncertainties in radiotherapy treatment planning by means of coverage probability. Int J Radiat OncolBiol Phys, 43:905-919.

[8]. Herman MG, (2005). Clinical use of portal imaging. Semin Radiat Oncol 15:157-167.

[9]. Langmack KA, (2001). Portal Imaging. Br J Radiol, 74:789-804.

[10]. van Herk M, Bruce A, Kroes AP, Shouman T, Touw A, Lebesque JV, (1995). Quantification of organ motion during conformal radiotherapy of the prostate by three dimensional image registration. Int J Radiat Oncol Biol Phys; 33 (5):1311-1320.

[11]. Ekberg L, Holmberg O, Wittgren L, (1998). What margins should be added to the clinical target volume in radiotherapy treatment planning for lung cancer. Radiother Oncol 48:71-77.

[12]. Tinger A, Michalski JM, Cheng A, Low DA, Zhu R, Bosch WR, Purdy JA, Perez CA, (1998). A critical evaluation of the planning target volume for 3-D conformal radiotherapy of prostate cancer. Int J Radiat Oncol Biol Phys 42(1):213-221,

[13]. Hurkmans CW, Remeijer P, Lebesque JV, Mijnheer BJ., (2001). Set-up verification using portal imaging; review of current clinical practice. Radiother Oncol 58(2):105-120.

[14]. Yan D, Wong JW, Vicini F, Michalski J, Pan C, Frazier A, Horwitz E, Martinez A., (1997). Adaptive modification of treatment planning to minimize the deleterious effects of treatment setup errors. Int J Radiat Oncol Biol Phys 38(1):197-206.

[15]. Bel A, Vos PH, Rodrigus PT, (1996). High-precision prostate cancer irradiation by clinical application of an offline patient setup verification procedure, using portal imaging. Int J Radiat Oncol Biol Phys 35(2):321-332,

[16]. Faiz M. Khan, (2003). The physics of radiation therapy, 3rd ed. ed. (Lippincott Williams & Wilkins, Philadelphia).

[17]. Karzmark J, Nunan C.S and E. Tanabe, (1993). Medical electron accelerators, (McGraw-Hill, Inc, Health Professions Division,).

[18]. Langen KM, Jones DT, (2001). Organ motion and its management. Int J Radiat Oncol Biol Phys; 50(1):265-278.

[19]. Balter JM, Sandler HM, Lam K, Bree RL, Lichter AS, ten Haken RK., (1995). Measurement of prostate movement over the course of routine radiotherapy using implanted markers. Int J Radiat Oncol Biol Phys; 31 (1):113-118.

[20]. Beard CJ, Kijewski P, Bussière M, Gelman R, Gladstone D, Shaffer K, Plunkett M, Castello P, Coleman CN. (1996). Analysis of prostate and seminal vesicle motion: implications for treatment planning. Int J Radiat Oncol Biol Phys; 34 (2):451-458.

[21]. Booth JT, Zavgorodni SF, (1999). Set-up error & organ motion uncertainty: a review. Australas Phys Eng Sci Med; 22 (2):29-47.

[22]. Crook JM, Raymond Y, Salhani D, Yang H, Esche B, (1995). Prostate motion during standard radiotherapy as assessed by fiducial markers. Radiother Oncol; 37 (1):35-42.

[23]. Dawson LA, Mah K, Franssen E, Morton G, (1998). Target position variability throughout prostate radiotherapy. Int J Radiat Oncol Biol Phys; 42 (5):1155-1161.

[24]. Melian E. Mageras GS, Fuks Z, Leibel SA, Niehaus A, Lorant H, Zelefsky M, Baldwin B, Kutcher GJ, (1997). Variation in prostate position quantitation and implications for three-dimensional conformal treatment planning. Int J Radiat Oncol Biol Phys; 38 (1):73-81.

[25] Padhani AR, Khoo VS, Suckling J, Husband JE, Leach MO, Dearnaley DP., (1999). Evaluating the effect of rectal distension and rectal movement on prostate gland position using cine MRI. Int J Radiat Oncol Biol Phys; 44 (3):525-533.

[26]. Karl Otto, (2008). Volumetric modulated arc therapy: IMRT in a single gantry arc. Medical Physics 35(1): p. 310-317.

[27]. Roeske JC, Forman JD, Mesina CF, He T, Pelizzari CA, Fontenla E, Vijayakumar S, Chen GT, (1995). Evaluation of changes in the size and location of the prostate, seminal vesicles, bladder, and rectum during a course of external beam radiation therapy. Int J Radiat Oncol Biol Phys; 33 (5):1321-1329.

[28]. Stroom JC, Heijmen BJM, (2002): Geometrical uncertainties, radiotherapy planning margins, and the ICRU-62 report. Radiother Oncol, 64(1):75-83.

[29]. Zimmermann FB, Molls M, (1997). Influence of organ and patient movements on the target volume in radiotherapy of prostatic carcinoma. Strahlenther Onkol; 173(3):172-173.

[30]. Malone S, Crook JM, Kendal WS, Szanto J, (2000). Respiratory-induced prostate motion: quantification and characterization. Int J Radiat Oncol Biol Phys; 48(1):105-109.

[31]. Dawson LA, Litzenberg DW, Brock KK, Sanda M, Sullivan M, Sandler HM, Balter JM, (2000). A comparison of ventilatory prostate movement in four treatment positions. Int J Radiat Oncol Biol Phys; 48 (2):319-323.

[32]. James A. Purdy, (2008). Dose to normal tissues outside the radiation therapy patient's treated volume: a review of different radiation therapy techniques." Health Phys. 95 (5), 666-676.

[33]. Patel R.R and Mehta M, (2002) Three-dimensional conformal radiotherapy for lung cancer: promises and pitfalls," Curr.Oncol.Rep. 4 (4): 347-353.

[34]. Michael G. Herman, Jon J. Kruse, and Christopher R. Hagness, (2000). Guide to clinical use of electronic portal imaging. Journal of Applied Clinical Medical Physics, Volume 1(2): p.39-42

[35]. Langmack KA, (2001). Portal Imaging. Br J Radiol, 74(885):789-804.

[36]. van Herk MP, Remeijer P, Rasch C, Lebesque JV, (2000). The probability of correct target dose: dose population histograms for deriving treatment margins in radiotherapy. Int J Radiat Oncol Biol Phys, 47(4):1121-1135.

[37]. Cedric X. Yu, (1995). Intensity-modulated arc therapy with dynamic multileaf collimation: an alternative to tomotherapy. Physics in Medicine and Biology 40(9):1435-1449.

[38]. Vera Gjervan, (2015). VMAT for small cell lung cancer. Retrieved from http://hdl.handle.net/11250/2352155.

[39]. Philip Mayles, Alan E. Nahum, and Jean-Claude Rosenwald, (2007). Hand book of Radiotherapy Physics: Theory and Practice. Boca Raton, FL, USA: Taylor & Francis.

[40]. Jane Barrett, (2004). On target: ensuring geometric accuracy in radiotherapy. Retrieved from https://www.ipem.ac.uk/Portals/0/Images/On target ensuring geometric accuracy in radiotherapy.

[41]. Timothy Deegan, (2015). Investigation of fiducial marker and soft-tissue image guidance techniques in prostate radiation therapy. Retrieved from http://eprints.qut.edu.au/82289/4/Timothy_Deegan_Thesis.pdf

[42]. George Felix Acquah, Magnus Gustavsson, Chris Osam Doudoo, Richard Kwabena Agbeve, Bernhard Schiest, (2014). Clinical use of electronic portal imaging to analyse tumor motion variation during a 3D-conformal prostate cancer radiotherapy using online target verification and implanted markers. Retrieved from http://ijcto.org/index.php/IJCTO/article/view/0204.4

[43]. Se An Oh, Ji Woon Yea Min Kyu Kang, Jae Won Park1, Sung Kyu Kim, (2016). Analysis of the Setup Uncertainty and Margin of the Daily ExacTrac 6D Image Guide System for Patients with Brain Tumors. Retrieved from http://journals.plos.org/plosone/article/citation?id=10.1371/journal.pone.0151709

APPENDIX A

Table A. 1: Individual set-up errors (Δ) acquired from patient 1-3.

Orthogonal Directions								
Patient 1			Patient 2			Patient 3		
Vert.	lat.	long.	Vert.	lat.	long.	Vert.	lat.	long.
0.4	5	-2.2	-2.7	2.3	-5	-1.3	-0.9	-5.5
4.1	5.2	-1.6	0.3	4	0.3	1.3	-2.7	-1.8
-1.9	0.9	-8.3	-6.2	1	-3.5	4	1.1	0.4
-6.6	-10.9	2.7	-5.6	3	-1.8	0.4	-0.9	-1.8
-0.3	-1.5	2.5	-2.8	2	0.5	-0.2	0.2	-0.2
0	-3.3	2.5	-5	0.3	0.3	2.2	-1.1	0.9
0.9	-4.1	3.4	-3	-3	0.7	-1.8	-2.4	-2.9
-2.7	-2.4	0.2	-5.9	-1	-3.3	0.2	0.2	1.1
0.3	2.4	0.5	-2.8	-17.3	-2.3	-2.4	-2	-0.9
-2.7	0.6	0.8	-5.7	-1.8	-2.8	1.8	-5.1	4.4
-1.8	-1.3	-0.2	-5.8	0.8	2.3	0.4	-3.8	5.7
-2.1	-2.9	0.9	-2.8	-0.8	-0.5	-0.4	-6	6.9
-2.7	-1.8	1.4	-5.1	-6.1	0.8	4.9	-5.1	6.9
-3.8	-8.5	-2.4	-0.8	0	0.5	0	-8	7.7
-1.8	-7.4	-2.7	-2.8	-6.6	-3.8	0	-6.2	1.8
-5.3	-5.9	-3.5	-6.6	-1.6	-2.3	-2	6	-2
2.7	2.9	1.5	-4.2	2.6	0.5	1.3	3.3	-1.8
-5.1	-1.1	0	-3.7	0.2	0	2	3.8	-0.4
-1.5	-2.2	0.7	2.7	1	-3	-0.4	6.9	-4.6
-4.6	-2	1.1	-6.2	-1	-3.7	1.7	5.6	-1.3
-1.8	-3.5	-1.5	-5.2	-0.7	-2.2	1.6	3.3	1.8
0.9	0.3	1.2	-3.2	-2.7	-0.2	0.3	6.2	4.5
-4.7	-2.3	-1.3	-10	3	-4	-2.6	5	-0.5
-4.1	1.4	-1.4	-5.3	3.1	-3.5	0.5	4.3	0.3
-0.7	-0.7	0.7	-6.4	1.5	-3.2	0.3	-5.3	-0.5
0	4.7	-2.5	-7.7	1.5	-6.75	4.1	-3.8	1
-6.5	0.3	-3	3.1	-1.1	-0.35	0	-4.3	0.3
-2.6	-1.3	-3.3	-0.4	-1.3	0.2	0.3	0	1.5
-2	2.7	-3.6	1.3	-0.2	0.1	7.8	1	2.7
-3.6	8	-5.7	0.4	-1.1	-1.8	1.8	2	1.3

Table A. 2: Individual set-up errors (Δ) acquired from patient 4-6.

Orthogonal Directions								
Patient 4			Patient 5			Patient 6		
Vert.	Lat.	Long.	Vert.	Lat.	Long.	Vert.	Lat.	Long.
-1.3	-2.3	0	-4.2	10.4	-5.7	2	-4.3	-3.3
0.3	0	-1.5	5.9	7.6	-3.7	3.6	-4.9	-3.9
-5.6	3.8	-10.6	-3	6.6	-4.6	3.9	-3.9	-3.5
-7.6	2.3	-11.1	3.5	5.9	-3.7	0.7	-2.5	-4.4
-5.7	-2.3	-9.3	1	1.2	-2.2	-4.2	-5.7	-9.4
-3.2	0.3	-3.1	-5.2	-15.3	-5.9	-4.7	-7.6	-8.1
-4.3	-2.5	-2	6.2	0.5	-3.9	-4.4	-4.7	-9.1
-1.8	-0.2	-3.7	11.1	-4.9	-11.1	-5.2	-6.2	-9.9
1	0.8	-1.5	10.4	-2.5	-11.6	-4.4	-5.2	-11.1
4.8	1.5	0.7	9.6	-5.4	-12.8	-7.5	-5.4	-5.9
-1	1.1	0	9.9	-3.5	-14.8	-4.9	-5.4	-10.1
1.6	3.3	1	-10.4	2	-6.4	-6.2	-6.2	-12.3
1.7	7.6	-4.7	-7.9	2	-6.9	-6.2	-10.4	-10.1
1.7	*8.1*	*-3.5*	-9.2	-1.3	-7.9	-4.9	-7.2	-9.6
5.4	-2	-1	1.6	-14.5	-1.8	-6.2	-8.1	-8.4
0.2	4.9	-2.5	-2	0	-2.3	-4.9	-2.7	-10.6
1.5	2.2	-2.7	-0.5	-1.5	-0.5	-4.2	-1.2	-10.9
-0.2	9.1	-1.5	1	-3	-2	-3.5	-1.7	9.4
2	3.9	-3.9	-3.2	-2	-1.7	-6.9	-0.7	-11.6
3.2	4.7	0.5	-4.4	0	-3.5	-1.5	-3.5	2
4.9	3.7	-5.2	0.7	-3.9	-3	-2.5	-0.2	0.2
-0.2	5.4	-0.5	-0.5	-1.5	-2	-2	-0.7	0
2.2	3.5	-2	-3	-2.6	-3.9	-0.5	0.2	0.7
-0.5	3.7	-4.2	-1.5	-2	-2.5	-0.5	-1	3.5
-0.5	1.7	-2	-1.3	-2.6	-4.3	-0.5	-0.5	0.2
-0.5	3	-7.2	0.3	-4.3	-3	-3.9	0.5	0.2
5.7	4.2	-4.2	-0.3	-4.3	-6.2	-1.2	-0.5	3.7
3	6.2	-6.9	-1.6	-2.3	-4.6	-0.5	3.2	-0.2
2.2	5.7	-5.2	-2	-7.9	-5.6	-1.5	2.7	-2.2
5.2	4.2	-2.2	0.3	-5.9	-6.6	-4.7	2	0.5

Table A. 3: Individual set-up errors (Δ) acquired from patient 7-9.

Orthogonal Directions (mm)								
patient 7			patient 8			patient 9		
vert.	lat.	long.	vert.	lat.	long.	vert.	lat.	long.
1.5	2	-1.5	-1.5	1	1.2	-3	-0.5	1.1
0.2	1.5	2.2	-2.2	2.2	2.5	-3	-1	1.3
-4.4	1.5	-0.7	-1.2	-1	2	0	4.4	0
-0.5	2.7	3.5	1.2	0	0.5	0	1.5	0
-3	3.9	-1	-0.2	0.2	3.5	-0.5	-0.5	1.3
-3.5	2.7	-3.7	-1.2	-1.7	-1.2	0	-0.5	1
-3.7	3.2	0.2	1	1	0.5	1.5	0	-0.2
-1.5	-1	1	-3.7	-0.7	-0.5	0	-1.5	0.5
-2.5	1	-0.2	-7.4	-0.5	-2.5	1.5	-3	1
2.5	-0.5	-0.5	-0.7	-0.5	0.2	2	-3.9	-1
-1.7	2.2	-3.7	-5.4	-0.7	-0.7	-1.5	-3	1.5
0	3.5	-3.5	-0.5	3.7	-0.7	-0.5	-1	0.8
-0.7	1.5	-3.9	-2.7	2.2	-0.5	-1	-3	0.3
5.2	3.2	-3.5	-3	0	0	1	-8.6	0.4
-2.7	2	-3	2	0.7	-0.2	-0.5	-1	0.5
-1.5	4.4	-2.2	-2	0.2	-2.5	-2.5	-1	1
4.9	4.4	-0.7	0.5	2.7	-3.2	0	0.5	1.3
-0.5	3.9	-2.7	-2.2	0.2	-2.5	-4.6	1	-5.3
3.7	6.9	-7.9	1	0.7	1.5	-2	1	-1.6
0	3	-3	-1.5	0.0.	-5.4	-1	-0.3	-2
-1.5	3	-4.7	0.2	2.5	-0.2	-1.6	-0.7	-1
0.7	3	4.7	1.2	3	-0.2	-2	0	-1
0.2	3.2	1.5	5.9	0.7	0	-1.5	3	-1.6
3.2	1.2	-0.2	-0.7	3	-0.2	-2.3	6.6	-7.9
1.5	3.7	-0.5	2.2	1.7	-3.2	-2.2	3	-6.2
2.5	4.7	0.5	0.2	3.7	-0.2	-6.2	3.3	-5.9
3.7	5.7	2.2	-1.2	1.5	-3.7	-7.6	4.6	-5.9
-3.9	-2.5	4.7	0.2	1.5	-3.5	-8.2	2.6	-5.3
-1.5	-1.2	4.4	-0.7	1.7	-2.5	-0.7	2.5	-3.5
-2.5	-0.5	2	0	0	1	-2.3	1	-3.6

Table A. 4: Individual set-up errors (Δ) acquired from patient 10-12.

Orthogonal Directions (mm)								
patient 10			patient 11			patient 12		
vert.	lat.	long.	vert.	lat.	long.	vert.	lat.	long.
0	1.6	-1	0	-0.7	-1.7	-1.2	7.6	3
3.9	-0.5	2	-3	1.5	0	-0.5	4.2	-2.5
-3	-3.9	-3.3	-0.5	0.2	-0.5	-0.5	6.7	-1.2
0.3	-1.3	-3.3	-0.5	-0.5	-0.5	-0.7	6.7	-3
0.3	2.3	-0.3	0.7	-0.5	-1.2	-2.2	0.595	0.0
-2	0.0	-2.5	-1	2	-2.5	-0.7	-3	1.5
1.5	-3.6	0.3	-3.5	-4.9	-2	-3	-2	-3.5
-1	1.3	-2	0.2	-8.1	-3.9	-1.2	-10.9	2.2
-0.5	-0.5	-2	-2.5	-4.7	-1.2	-3.2	-2.7	-1.5
2.5	-2.5	-3	3.9	-3.9	-3.7	-0.5	-2.5	0.2
1.7	1.5	-13.1	-2.7	-1.7	-2.7	-3.2	-3.2	0.6
0.5	0.7	-14.6	0.0	-3.5	-4.4	-3.7	-2	-2.7
-3.6	4.3	-9.2	-0.2	-6.7	-3	-3.5	-2.2	-1.5
0	1.6	-7.6	-1.7	-2.5	-1.7	1.2	-2.2	0.5
-5.3	0.3	-12.8	-3.2	-3.5	-5.2	3.2	-3.5	2.5
-9.9	0.7	-12.6	-3.2	-2.2	-6.7	0.2	-3	0.7
-7.6	0.3	-12.5	-1.2	-6.2	-3.5	3.2	-0.5	2.2
-5.1	0.3	-12.8	-2.2	-3.5	-2.7	5.7	0.2	-3.7
-6.9	-1.7	-9.1	1.2	-2.7	-2	-5.9	-3.5	3
-7.6	-0.3	-10.2	-8.1	-7.4	-5.4	0	-3.2	1.2
-0.3	1.6	-2.3	1.7	-4.7	-6.9	-1.2	-1.7	-0.2
-1.5	0.7	0.3	0.2	-5.2	-2.5	0.2	-4.7	-0.7
3.5	1.3	0.7	-6.7	-7.9	-7.4	-1.5	-1.5	1.5
0	1.2	-3.2	-2.2	-7.2	-4.9	5.4	-1.7	2
-0.3	-1	-0.3	-3.5	-8.4	-5.4	3.5	-3.7	1
1.5	3.2	5.2	0.5	3.2	-1.5	4.4	-4.2	3
1	2	4.4	1.2	3.7	1.2	2.5	0.7	5.4
1	2.5	2.5	-2	0.5	-0.5	3.5	-3.9	2.2
0.2	-2	0.2	0.7	0.7	1	3	-4.9	3.2
0.5	3.5	-1.2	0.7	1.2	-5.7	-3.5	-5.2	2.7

Table A. 5: Individual set-up errors (Δ) acquired from patient 13-15.

Orthogonal Directions (mm)								
patient 13			patient 14			patient 15		
vert.	lat.	long.	vert.	lat.	long.	vert.	lat.	long.
-1.7	-5.9	3.7	0.2	1.5	1.5	1	1	0.5
2.7	-5.2	2	-0.5	1.5	1	-3.7	-0.7	-0.5
1.5	-4.4	3.5	3.2	3	0	-7.4	-0.5	-2.5
0.5	-0.7	3.2	0.7	1.2	0.5	-0.7	-0.5	0.2
-5.4	-3.5	3.7	1	-0.2	-1.7	-5.4	-0.7	-0.7
-2	-4.2	5.7	2.3	3.3	-0.3	-0.5	3.7	-0.7
-3.2	-4.2	3.7	0	2.5	2	-2.7	2.2	-0.5
10.4	2.7	0	5.2	3	-2	-3	0	0
10.9	0	7.4	0.2	3.2	0.2	2	0.7	-0.2
0	-3.2	3.5	2.2	6.2	2	-2	0.2	-2.5
0.5	-3.7	7.6	4.9	-0.2	-2.2	0.5	2.7	-3.2
-6.5	-4.2	3.2	2	-2.7	0	-2.2	0.2	-2.5
-3	0	0	4.9	0	-0.7	1	0.7	1.5
1.5	2	3.9	5.4	-3.9	2.2	-1.5	0.0.	-5.4
1	3.5	3.9	5.4	-3	1.5	0.2	2.5	-0.2
2.5	2.5	0.5	2.7	-0.5	-1.5	1.2	3	-0.2
-2	3.3	0.3	3.5	-1.7	0.7	5.9	0.7	0
-1.5	4.2	2	0.7	-3.5	-5.7	-0.7	3	-0.2
-1	4.4	-0.2	7.6	-3.7	2	2.2	1.7	-3.2
-0.7	5.9	2.7	4.4	-10.4	-0.2	0.2	3.7	-0.2
0.7	3.2	-0.2	7.6	-2.5	-0.7	-1.2	1.5	-3.7
1	3.9	1	-3.9	-2.5	4.7	0.2	1.5	-3.5
1.7	0	1.5	-1.5	-1.2	4.4	-0.7	1.7	-2.5
-2.2	0.7	-3	-2.5	-0.5	2	0.2	-1	-2.7
1	-0.2	2	-1.5	1	1.2	-2	1.2	-1
-0.5	1.2	2	-2.2	2.2	2.5	6.2	0.2	0
2	2.5	2.7	-1.2	-1	2	2	1.2	0
2	1	-0.2	1.2	0	0.5	0.2	0.5	-2.2
2.7	1.7	2.2	-0.2	0.2	3.5	3.5	1.7	3
0.5	0.2	-1.2	-1.2	-1.7	-1.2	-0.2	3.2	-3.5

Table A. 6: Individual set-up errors (Δ) acquired from patient 16-18.

Orthogonal Directions (mm)								
patient 16			patient 17			patient 18		
vert.	lat.	long.	vert.	lat.	long.	vert.	lat.	long.
0	7.6	2	3	-4.7	-0.7	1.0	1.0	2.0
3.5	6.4	2.2	2.7	-9.1	-1.2	8.4	5.4	6.4
-0.7	6.7	2.6	5.4	-6.7	-2	-2.0	10.9	-1.5
-4.2	-0.5	-0.5	4.2	-6.9	-1.7	1.0	8.4	-0.5
0.7	-5.9	0.7	0	-7.6	2	-1.5	18.7	-3
1.7	-4.9	2.7	6.9	-4.9	-2.2	3.9	9.9	-0.5
0.5	-3	0	-0.5	-1.5	0	4.4	6.4	3
3.5	0.7	1.7	4.2	-5.4	0	0.0	8.4	2.5
0.2	-2.2	3.7	0	-5.7	-1	2.5	20.2	1.5
3	-1.7	-3.7	18.7	9.5	-0.3	-5.9	-8.4	-6.4
2.5	-3.5	1	13.3	10.4	1.8	1.0	17.3	7.4
-1.2	-3.5	-1.7	15.3	7.4	-3.7	1.0	3.9	4.9
0.2	0	3.5	3.5	1.5	2.3	-2.5	12.3	5.9
-0.5	-2.7	-0.5	-7.2	4.4	-5.7	-1.0	-4.6	3.6
1.2	-4.7	-0.5	-8.9	0.2	-5.4	-0.5	3.9	2.5
-1.2	-3.7	-1.7	-5.9	-1	-3.5	0.0	11.8	2
2.2	-6.2	-1.2	-5.4	4.4	-2.2	-4.2	9.1	1
-1	-8.6	0	-4.2	-1	-2.5	-2.0	8.4	2
-0.5	-8.6	0.4	-0.7	2.2	-6.2	1.5	20.2	3.2
0.5	-7.4	0.2	4.2	2	-8.1	1.2	19	4.9
1.5	-11.8	1	-5.2	2.7	-3.9	-0.7	-2.5	5.9
6.9	-8.4	-1.7	-4.2	2.7	-1.7	3.0	-6.2	9.6
2.2	-8.9	-1	4.4	3.9	-6.9	5.9	22	6.2
1	-5.9	0.5	-6.4	3.6	-3.6	0.2	21.7	5.7
-2.7	-8.9	0	-4.4	2	-6.4	2.5	16.3	6.7
-1.2	-2.7	-2.2	-2.5	2	-5.7	6.4	3.9	2.7
3.5	-1.5	1.5	-5.7	3.7	-3.9	5.7	5.2	3.2
1.5	-2.2	0.2	-0.2	3.2	-4.9	3.0	5.9	1
0.5	-1.2	-1	-4.7	3.5	-4.9	-2.8	0.2	-2.3
1	-3.7	0	-3.6	3.9	-5.9	1.0	0.0	0.0

Table A. 7: Individual set-up errors (Δ) acquired from patient 19-21.

Orthogonal Directions (mm)								
patient 19			patient 20			patient 21		
vert.	lat.	long.	vert.	lat.	long.	vert.	lat.	long.
0.0	1.7	-0.5	-3.0	4.9	3.9	-0.5	3.9	2
0.2	1.2	0.0	-3.5	5.4	3.9	0.0	-4.4	3.5
2.7	2.5	-0.5	-3.0	5.4	2	0.0	-1	0.5
-1.7	0	0	-1.0	1	1.5	0.0	2.5	0.5
-0.5	-0.2	1.7	-3.0	1.5	3	0.0	-6.9	0
1.0	3.5	4.7	-2.0	4.4	3	0.0	4.4	2.5
0.0	0	1.5	-0.7	3	0.5	-1.5	1.5	-1.0
1.7	4.7	7.4	-2.0	5.9	2	-4.4	1.5	2.0
1.2	1.5	1	0.0	0	0.5	-3.0	0.0	0.0
-3.0	-5.4	-2.2	-3.5	0	4.9	-1.0	0.5	3.2
0.0	-3.5	0.0	0.0	-3.5	0.5	-4.9	-0.5	3.5
0.0	-3.0	0.5	1.5	-0.5	41.7	-1.5	0	0.4
	0	-6.4	0.5	1	3.3	9.9	-1.5	0
-0.5	-1.5	-2	0.7	-3	3.5	-2.5	0	-1
2.5	-4.4	-4.9	-1.0	-1	2.7	0.0	0	6.9
0.0	-2	-6.4	0.0	0	0	0.0	2.5	-1
-0.5	-6.9	-3	-0.7	0	-0.5	0.5	7.4	3
0.5	0.5	0	0.0	-2.2	1.7	-2.5	0	0
0.0	0	-6.9	-2.7	0	0	0.0	-0.5	0.5
0.0	-3.9	-1	0.0	-0.2	0.5	-6.4	2	0
1.5	-2.5	-1.5	0.0	2.0	2.5	-6.9	5.9	1
-1.0	-5.4	-4.4	-3.5	3.0	3.9	-1.5	3.5	-1
2.5	-11.3	-3	1.0	4.4	2.0	-2.5	1	-0.5
2.0	-0.5	1.5	-2.0	5.9	1.5	-3.0	5.9	1.5
-0.5	4.9	-7.9	0.0	-3.5	1	-3.0	-5.9	7.4
-1.5	1.0	-10.4	0.0	6.9	0	-2.0	10.4	3
4.4	3.5	-11.8	-2.5	-6.9	2.5	2.0	3.9	6.5
3.5	1	-7.9	0.0	8.9	-0.5	1.5	0.2	1.2
-6.9	0	3.9	-0.5	9.9	4.4	-1.5	1	0.2
1.2	-3.2	0.5	0.0	-2	0	-0.7	3	5

Table A. 8: Individual set-up errors (Δ) acquired from patient 21-24.

Orthogonal Directions (mm)								
patient 22			patient 23			patient 24		
vert.	lat.	long.	vert.	lat.	long.	vert.	lat.	long.
-1.2	2	1.5	-2.7	0.2	2.5	-4.4	-1	3.4
-1.7	0	0.2	2.7	1	1.2	2.0	-1.5	4
-4.9	0.5	3.3	-0.2	1.2	2	-2.0	0.5	1.5
-0.7	4.2	5.4	-1.2	-0.5	2.2	-1.0	0	0
-1.2	1.7	3.6	1.2	-1.7	-4.2	-2.5	0	1.5
-2.0	13.6	2.5	0.3	-1.2	-3.2	2.0	0.5	1.5
-4.4	-1	3.5	-3.5	0	2.2	-2.5	-20.2	-8.9
-3.0	1.7	3.1	2.0	-0.7	2	-0.5	-0.5	3.7
-3.7	-2.2	0.5	1.7	0	6.3	-4.4	1	1
-4.2	4.7	5.2	0.5	-1.5	-1.2	4.9	-3	9.1
-7.2	1.2	1	-0.5	-1.5	0.5	-3.5	0.5	8.9
2.7	3.9	1.7	-1.5	-1	1.2	-5.9	1	6.7
-2.2	0.5	0	1.0	0	0	0.2	0	6.4
-0.7	2.0	0.0	0.2	-1.2	-1.7	-4.7	-1.2	5.9
1.0	-1.3	-1.3	0.0	1.2	-0.7	-3.2	-3.7	0
0.0	-1.5	-2.7	0.0	0.5	-2	-7.6	-0.2	4.4
-3.3	-1	2.2	0.0	0	0	-5.7	-0.2	6.4
-0.7	-0.7	0.2	1.5	-6.9	-6.4	1.7	-0.7	4.7
0.5	1.5	0.7	1.0	0	0	-0.5	4.4	3
-1.5	0	0	-2.5	1.5	3.0	4.2	0	-1
0.2	-2.5	1.2	-3.9	1.5	0.0	3	-2	0
0.0	-1.2	0.5	-1.5	2.5	1.5	3.2	-0.5	0
-0.2	-2.2	0	0.0	0	0	-0.7	0.5	-2.2
0.0	0.3	1.3	-3.0	1.5	3	-2.2	1.5	-0.2
-0.7	-0.5	1.2	-3.9	1.5	0	4.4	0.7	1.5
-2.7	-0.2	0.2	-1.0	2	1	-3.5	0.2	-2.5
1.0	-1.6	0	-6.9	0	0	-0.2	2.6	-2
-5.4	3.5	0	-4.4	0.5	4.9	-1.2	-1	-1.6
-1.2	0.5	1.7	-2.0	0.7	1.6	-2.2	1	-1
-0.2	0	0	-3.5	3	2	-3	-2.5	-0.2

Table A. 9: Individual set-up errors (Δ) acquired from patient 25-27.

Orthogonal Directions (mm)								
patient 25			patient 26			patient 27		
vert.	lat.	long.	vert.	lat.	long.	vert.	lat.	long.
-2.3	1	2.7	0.0	2	-5.4	0.0	-2.3	0
-0.7	0.2	0.7	-5.9	4.4	-6.2	3.9	-1.6	3.3
-4.2	-2.5	4.7	3.5	1.2	-2.7	0.7	-10.5	-0.7
1.5	2.5	2.7	-4.6	-3.6	-3.9	-2.0	-3.9	-2.7
3.9	1.7	7.2	-8.4	4.4	-6.7	-2.0	0.2	-0.5
-3.9	2.0	-9.5	-8.4	1	-4.7	0.2	2.2	2.5
-19.2	-3.0	-18.3	-3.0	-1	-2.2	3.0	-8.9	-1
-14.3	-2.0	-1.5	0.0	-0.5	-0.5	-2.5	-2.7	-1
-6.9	1.5	-3.7	-5.4	4.7	-4.2	5.4	-5.7	1.9
-14.5	-5.9	-19.7	-0.5	0	4.4	-0.7	-0.5	-0.5
-9.9	0	0	-4.9	-2.7	-7.4	2.2	0	0
-9.9	-0.5	-3.9	0.5	0.5	0.0	-0.2	-4.9	1
-4.9	1	-5.4	-3.0	1.7	-0.5	-0.2	2.6	0.2
5.9	2	-5.4	0.2	0.7	1.7	-1.0	-3.2	-1.7
-5.9	19.2	-5.9	0.7	5.9	0	1.2	4.4	1.5
5.4	-1	-7.4	-0.7	3	0.7	3.7	-4.2	2
-9.9	1	0	1.0	-0.2	0.5	2.5	-9.4	0
-7.9	-0.5	-7.4	1.0	-1	0	6.2	3.5	-5.9
-9.9	-1	-2	0.0	-0.7	0	8.6	-1.7	-5.9
-3.0	1.5	0	0.0	-1.5	0	4.2	1.0	-7.2
-10.4	16.3	-8.4	2.2	0.2	0	4.4	0.5	-8.4
-2.0	0.5	-2.9	8.9	-2.7	4.9	3.0	-0.7	-8.9
-5.4	-0.5	0	6.9	4.4	5.2	6.9	5.2	-5.4
-2.5	-0.7	-0.3	-0.7	-5.7	-1	1.5	4.9	-2.2
-0.5	1.6	-8.6	0.0	-2.7	0	10.6	4.4	-2.2
-6.9	3.5	-3.7	5.9	-1.7	2	3.5	2.2	-6.2
-8.9	0.5	-5.3	0.5	5.4	0	1.0	-2.7	-8.2
-0.7	1.6	-5.6	2.5	-2.5	0.2	3.7	8.6	-8.6
-6.4	-1.6	-4.9	0.7	-5.4	0	7.4	6.2	-6.2
-7.6	3.7	-4.4	2.5	1.7	0	3.0	2	-5.4

Table A. 10: Individual set-up errors (Δ) acquired from patient 28-30.

Orthogonal Directions (mm)								
patient 28			patient 29			patient 30		
vert.	lat.	long.	vert.	lat.	long.	vert.	lat.	long.
5.9	2	-10.1	1.0	8.3	2.7	-0.7	4.2	2.2
5.4	4.2	-6.4	2.7	0.2	2	0.0	0.7	0.0
-1.2	3	-7.9	-1.5	-5.2	-1.2	2.2	1.5	0
2.5	2.7	-7.9	7.9	0.2	7.2	-6.4	1.2	-2.1
4.4	-1.5	-6.2	5.2	3	-3.2	-3.9	6.9	0.5
3.9	2	-19.7	7.2	0.7	0.2	-2.5	4.4	-0.7
5.7	0.7	-0.7	3.0	2.5	-5.2	-0.7	5.4	-1
9.1	3.2	-6.9	3.5	4.2	0	-4.4	2.7	4.7
6.2	-0.5	-2.5	-0.3	-5.3	10.2	-6.4	3.5	1
6.4	0	-1.5	-0.2	-1.5	0.5	-3.6	-6.9	2
0.0	1.7	-0.2	-1.5	3.9	-14.3	-4.9	-0.5	1.2
7.6	-1.5	2.7	6.4	0	0	3.5	2.5	0
1.0	-1.7	-4.5	0.2	0.2	-1	0.7	-7.4	2.2
5.4	3.9	-7.4	3.2	4.9	2.2	-1.5	-2.2	-1.7
3.5	-0.2	0	0.7	1.7	0	-5.9	0	-1
8.6	3	-4.4	2.5	-1.2	-0.2	-3.7	5.2	0
2.2	2	-1.7	8.1	0.5	0.5	-2.5	0.5	1.5
1.7	-1.2	0	0.2	0.5	2	-4.2	1.7	-1
0.0	4.9	-2.5	6.2	0.7	1	-1.0	-0.5	1.2
1.2	0	-2.2	2.0	0.2	-0.2	-2.2	2.5	-3.3
-0.7	2.2	-7.5	0.7	-1.7	1.2	0.5	0	0
7.2	2.7	-5.2	1.0	1.2	0.2	3.9	1.7	0
5.9	0.2	4.9	-1.0	-0.2	0.5	-0.2	1	2
0.7	2.7	0.0	0.0	1.7	0	0.0	1.7	0
0.2	2.0	3.5	6.2	0	0	1.7	0	-0.5
4.4	0.0	0.0	1.7	1	-0.2	-7.4	3.5	-3.2
2.7	-0.5	-1	-0.2	0.7	0	-4.2	0.7	1.2
3.5	2.2	3.5	2.7	-0.5	1.7	3.2	-1	2.5
6.4	0.7	0	-0.5	1	0	-7.4	-2	0.2
5.4	2.7	3.4	7.2	1.7	0.7	-3.7	-3	1.5

Table A. 11: Individual set-up errors (Δ) acquired from patient 31-33.

Orthogonal Directions (mm)								
patient 31			patient 32			patient 33		
vert.	lat.	long.	vert.	lat.	long.	vert.	lat.	long.
-7.9	9.9	-12.1	-3.3	-2.6	0	3.2	2.5	3
-1.7	1.5	-0.5	-1.3	-7.2	-2.6	-0.5	3.2	11.1
-12.1	-4.9	0.7	6.2	-0.7	1.2	3.7	-1.2	7.3
-0.7	0	0.5	6.2	6.2	1.5	0.0	4.2	4.5
-5.7	-2.7	1.5	-3.7	-1.7	-4.9	9.1	0.7	0
1.0	3.6	1.3	1.5	-3.2	4.4	3.0	4.2	-2.7
-1.0	4.9	-7.4	7.6	1.5	5.2	10.4	3.7	4.4
-4.9	-2.0	-5.5	-1.7	-1.2	3.5	0.7	8.6	2.2
3.3	3.6	-2.3	3.7	8.9	3.9	-4.4	3.5	-6.2
-2.0	5.9	-3.6	2.2	-3	-1.7	3.0	9.4	-5.1
0.0	5.9	0.5	-4.9	-0.5	2.5	2.0	0.5	0.0
-5.3	-0.7	-1.3	5.7	-0.7	4.2	2.5	6.9	-8.4
-3.2	2.6	17.8	-2.5	-5.7	2	-1.5	6.9	2
1.3	3.6	0.7	0.0	-3.7	2	4.9	10.4	-6.9
-4.7	-2.3	-2	3.5	-0.7	-0.7	5.4	6.4	6.4
-3.2	-1.5	-4.5	-7.4	2.5	4.2	5.4	11.8	-3.7
-4.3	3.7	-3.9	3.9	-3.9	3.5	1.0	8.9	-4.7
-1.0	0.7	-9.9	2.0	1.7	4.9	-1.0	10.9	-2.5
6.4	7.9	-7.2	2.0	0	2	2.0	9.4	-6.4
0.0	-1	0	5.9	4.9	4.4	0.0	10.4	1
0.0	1	-1.6	-3.2	1.2	3.5	1.0	-16.8	1.5
6.6	6.9	-4.6	4.2	-1.7	3.9	4.4	12.8	10.9
1.6	7.6	1	3.5	4.4	2.2	0.0	7.4	1.5
0.0	-0.7	0	2.2	-4.2	4	0.0	-2.5	0
-1.3	-2	0	6.2	-2.5	0	-3.0	9.4	1
2.0	1	-2.5	6.9	-2	-1	0.5	4.9	1
-1.6	12.8	-5.7	-2.2	8.1	-3.5	-0.7	8.9	-1.2
-5.6	-2.5	-4.7	6.9	2	1.7	1.0	13.3	2.9
1.5	5.7	1	4.9	-10.4	-4.7	-0.2	-7.6	-2.2
1.5	2	-7.6	0.2	-4.9	-6.1	-0.7	0.5	0.5

Table A. 12: Individual set-up errors (Δ) acquired from patient 34-36.

Orthogonal Directions (mm)								
patient 34			patient 35			patient 36		
vert.	lat.	long.	vert.	lat.	long.	vert.	lat.	long.
-3.0	-14.3	0	-1.0	-0.5	1	-1.2	13.8	1.2
0.0	4.3	-1.6	0.0	0	2	-1.2	2.2	1.6
0.2	3	2.2	-2.5	3	1	-1.5	3	3.9
0.5	0.7	-10.4	-1.0	-0.5	2	1.0	2.5	-1.7
-1.5	-1	-2.6	0.0	-1.5	0	-3.9	14.6	0
0.0	6.2	-4.4	1.5	0.5	1.5	-3.9	2.7	-3
-1.0	-3.7	-1.2	6.2	3.5	0.0	0.0	4.4	-4.5
-1.0	13.6	0.2	-2.5	9.4	-2.0	-1.0	6.2	-3.5
0.0	1.7	-0.7	-4.9	0.0	-2.0	-1.5	3	-2.2
0.0	-1	-1.7	-11.3	-2.5	10	0.0	5.9	-0.5
-0.7	8.1	-4.7	-4.9	0.5	8.4	1.2	0	0
1.2	2	0	-11.8	4.9	-5.6	0.0	8.6	-3
1.7	-1.3	-4.5	-6.4	1.5	-1	0.0	4.2	-3.9
-3.9	-1.0	-1.0	-6.9	2.5	7.4	2.5	-0.5	-9.9
-5.4	0.0	0.0	-1.0	3	-1	-3.0	0.0	-1.7
0.0	0.0	0.0	-5.4	0.5	2.3	-3.0	0.5	-5.9
0.0	0	0	-6.9	5.4	-6.2	-3.5	-0.5	-11.1
0.0	0	0	-6.9	3	-5.9	-2.5	0	-14.3
0.0	-3	0	-9.4	5.4	1	-3.9	-0.5	-4.5
0.0	0	0	7.2	8.1	-2.2	-7.9	0	-8.4
4.9	-0.5	0.5	-1.5	2	3.5	-3.0	-1	-11.4
0.5	0	2.5	-4.7	-0.7	-4.2	0.0	0	3
-2.0	0	3	-1.2	0	-2.2	0.0	0.5	-5.4
4.4	0	1.5	-1.7	10.1	-29.9	0.0	-0.5	2.5
-2.5	-0.5	1	0.5	1	-3	-8.9	1.5	4.4
0.0	-2.5	0	0.5	6.7	3.5	-7.9	0	-11.3
-1.5	-3.5	0.5	0.0	3	0	-6.9	0	3.5
-1.2	0	-0.2	-1.5	3.7	4.1	-2.0	-1	-4.9
0.0	0	0	2.0	7.4	3.9	-5.4	-1.5	3.5
2.0	0	2.5	-3.5	6.4	-3.5	-2.0	2	3

Table A. 13: Individual set-up errors (Δ) acquired from patient 37-39.

Orthogonal Directions (mm)								
patient 37			patient 38			patient 39		
vert.	lat.	long.	vert.	lat.	long.	vert.	lat.	long.
2.0	2.5	1	-6.4	13.3	7.9	0.7	4.2	1
-3.5	-1	-12.8	5.4	-12.3	13.3	1.0	-2.2	0
2.5	0	-1.5	8.4	11.3	-3	0.5	-5.4	2.7
-4.9	-1.5	-2.5	6.9	-16.8	2.7	4.7	-3	-2
0.0	0.5	1.5	3.5	0	-0.5	2.5	0	0
3.5	-1	-11.3	0.0	6.4	-12.3	-4.2	1.7	-0.5
0.0	0.5	0	-4.9	8.4	-8.4	11.3	-15	5.4
2.0	-0.1	-5.7	-4.4	5.9	-11.8	2.0	-6.7	3.5
-2.0	2	-5.5	0.5	1	0	5.2	5.7	-1
0.0	2	-2	-6.4	6.9	-6.4	0.5	-1.2	-2.7
0.0	-1.5	5.9	-4.4	8.4	-4.9	-1.5	-3.7	0.7
1.0	7.9	2.0	-3.5	3.5	-7.4	-5.9	-5.2	2.7
-0.5	-12.8	5.4	-5.4	6.4	-3.9	-0.7	-3.5	1.5
0.0	-13.8	0.5	-3.5	8.9	-4.4	-3.7	-2.2	4.4
0.0	-3.5	3	-2.5	4.4	-0.5	2.5	4.7	-3.5
-2.0	1.5	6.9	-1.5	4.4	-1.5	-2.0	1	4.2
7.9	-9.4	1	-6.4	3	0	-2.5	-3.2	-0.2
0.0	-22.2	4.9	-3.9	6.4	-5.9	-1.0	-0.2	6.2
-0.5	-18.7	3.5	-6.9	9.4	-6.4	2.5	1.2	3.5
-0.5	-18.3	6.4	-9.9	5.9	-4.4	-0.7	-0.2	2.7
3.0	-16.3	3.9	-1.3	4.9	-3	-2.7	-8.4	0.2
-3.5	-10.9	12.3	-6.4	8.9	-4.9	-2.0	-3	-1
-2.0	-12.8	10.9	-1	9.9	-4.9	0.0	-1.7	3
1.0	-8.4	7.7	-4.9	6.4	-5.4	0.0	5.4	0.7
-2.5	-6.4	3.9	3.5	1.7	0.5	-1.7	-2.2	-1.5
1.0	-20.7	7.2	3.0	0.0	0.0	-2.5	-2.2	-4.9
-4.4	-9.4	8.4	2.7	0.0	-1.2	3.0	4.2	-2.7
-2.0	-10.9	10.4	1.2	3.5	4.9	-2.0	-4.4	-0.2
0.0	-8.9	-4.4	2.7	-3.5	0.5	2.7	-3	3
1.5	-8.9	18.7	2.2	2.2	2.5	2.2	-5.7	-16

Table A. 14: Individual set-up errors (Δ) acquired from patient 40-42.

Orthogonal Directions (mm)								
patient 40			patient 41			patient 42		
vert.	lat.	long.	vert.	lat.	long.	vert.	lat.	long.
4.9	0.0	4.4	-4.4	0	2	3.0	-7.4	-1
-1.0	0.5	2.0	6.4	-11.8	-3	-1.0	-10.4	1.5
3.0	6.4	3.0	5.9	-1	3.5	-3.5	-4.4	9.9
2.0	-3	0	2.5	-10.9	10.9	-0.5	-14.3	3
1.0	-6.4	0.5	3.5	-9.4	14.3	0	-11.3	8.9
0.0	-1.5	2.5	-3.9	-12.5	6.9	-3	-14.8	2.5
2.0	4.4	5	0.5	-12.8	7.4	0	0	-3.5
-1.5	-1	1.5	0	0	14.3	-3.9	-12.3	-3.9
0.0	0	0	-2.5	-14.3	7.4	-2.5	-11.3	1.5
-1.5	-4.9	4.9	-0.5	-7.9	6.9	-1	-13.3	6.9
-3.0	-5.4	2	0.5	-10.4	2.5	-0.5	-13.3	1.5
0.0	-10.9	3	-3.5	-11.3	6.4	-1.5	2	4.4
-4.9	-3.9	3.9	-3.9	-8.4	1	3	-3	1
-1.0	0.5	3.5	0	-15.8	12.3	-1	-3	1
0.0	2.5	-2.5	-1	-8.4	0	6.4	22.7	4.9
5.4	-3.9	1.5	-2	-13.3	-1	1	-9.9	-4.4
2.0	1	1.5	-3	-15.8	-2	17.3	-3	5.9
2.7	-10.9	2.5	-2	-14.8	1.5	-3	-2	2
6.2	6.2	3.5	-2	-16.3	-1	5.9	3	-1
5.9	0.7	4.9	-5.4	-13.3	-4.9	3	-2.5	3.9
4.2	-0.3	3.6	-0.5	-18.3	1.5	6.5	-5.5	1.4
0.5	1	5.7	2	-10.4	3.5	9.4	3.5	0.7
-0.7	-3.7	1	0	-10.9	-4.4	3	2	0
3.5	-9.9	4.9	-3	-13.3	0.5	-0.2	5.7	14.1
-2.0	-6.7	3.2	-5.9	-7.4	0	-13.6	2.5	-3.9
7.4	-5.3	7.2	-0.5	-13.5	-0.5	0.0	1.2	-1.2
0.7	6.7	3.5	-5.4	-14.3	1	-2.0	1	-0.2
0.0	0	1.7	-4.9	-22.7	-3	-0.5	-0.5	4.7
-1.2	-0.2	3.2	0.0	4.9	-2	-13.8	0.5	-4.9
-5.9	-7.9	3.7	-1.5	-8.9	0.5	-5.9	5.4	-4.2

Table A. 15: Individual set-up errors (Δ) acquired from patient 43-45.

Orthogonal Directions (mm)								
patient 43			patient 44			patient 45		
vert.	lat.	long.	vert.	lat.	long.	vert.	lat.	long.
-3.9	-7.2	-6.9	1.5	9.4	-2.8	1.5	6.4	-3.5
-3.7	2	-2.5	4.4	1.0	1.2	-4.2	-0.7	-10.9
-6.4	5.7	-6.2	-1.0	-5.9	0.5	3.9	-1.2	-1.7
-6.9	5.7	-8.1	-1.0	-5.4	8.4	0.2	12.1	-1.5
-11.6	-8.1	-1.5	0.5	-0.5	8.4	-3.0	3.5	-1.2
-1.7	-5.2	-2.2	-2.0	-1	6.9	0.5	1.5	2.5
0.0	2.7	-3	-3.0	0.5	5.4	-3.5	0	2.7
-0.2	3.2	0.2	-4.4	-4.9	5.2	-3.2	-3.5	6.2
-2.5	1.5	-3.9	-6.9	1	4.9	-1.0	10.1	-3.5
-3.5	5.2	-4.7	-3.3	-8.4	6.9	2.5	5.7	4.9
-1.0	8.9	0	4.4	-5.9	-9.9	1.2	7.2	5.2
-2.7	1.7	0.2	-2.5	-4.4	9.9	-0.7	3.7	4.2
-11.8	-6.2	-3.7	0.0	-6.4	10.9	3.7	-2.5	-0.7
-6.7	2.7	-5.9	-0.5	-15.3	10.9	-2.2	0	2.2
-4.4	3.7	-1.5	-3.9	-12.8	9.9	-0.5	-0.2	4.2
-10.1	1	-5.9	-2.0	-4.9	5.2	-2.0	0	0
-8.6	2.2	-5.9	2.0	-2	7.4	-0.2	0.5	3.9
-8.1	3.2	-7.6	-4.4	-11.3	14.1	5.7	0.2	6.9
-11.6	14.1	-17.8	0.0	-8.4	-9.4	-1.0	1	-2.3
-9.6	-4.2	0.7	-2.0	-2	-6.9	2.5	-3.5	7.2
-13.1	6.2	-11.8	-1.0	0	-3	0.5	34.5	7.9
-3.9	1.2	-3	3.5	1.5	-1	-4.2	15.8	4.2
-3.9	2.5	-1	-1.0	1.5	0	2.2	2.7	4.7
-6.7	0.2	-7.2	1.0	-4.4	-4.9	4.4	-2	4.4
-14.6	-6.4	-5.9	3.5	-9.4	0.5	7.6	-1	13.6
-6.7	3.2	-4.2	-1.0	-0.5	6.4	-6.7	6.2	-4.4
-9.6	-4.7	-10.9	-2.0	1	0	-0.5	-0.2	10.4
-6.9	-4.7	-2.2	-2.5	-1	2.5	-2.2	1.7	6.4
-7.9	14.8	-14.1	-0.5	3.5	-5.9	4.7	15.8	4.7
-9.4	-0.5	-0.7	-3.0	-2.5	-1	7.4	11.6	3.5

Table A. 16: Individual set-up errors (Δ) acquired from patient 46-48.

Orthogonal Directions (mm)								
patient 46			patient 47			patient 48		
vert.	lat.	long.	vert.	lat.	long.	vert.	lat.	long.
3.0	-11.1	0	-3.0	3.9	-1.2	0.0	-0.5	0.5
6.2	5.4	-0.7	-1.7	0	0	0.5	1	-4.7
1.2	-1.5	3	2.7	2.2	0	1.5	1.2	-0.2
5.7	-1.2	4.7	0.0	0.2	6.7	2.2	1.5	-7.2
4.9	-5.2	4.7	0.0	3	-0.2	-1.2	0.2	-7.4
8.4	-14.6	7.9	2.0	-3.9	0.2	-2.0	3.9	0.5
-2.7	5.2	-4.2	-3.0	1	-2.2	-0.7	1	0.7
0.7	3.0	5.2	-0.2	0.2	-0.7	0.2	-1.2	1.7
1.5	-0.5	-1.5	-2.0	0	0	1.7	0.2	-2.2
-0.5	0.0	0.0	0.0	3.7	-2.2	0.0	-0.2	7.6
1.2	4.2	-1.2	0.7	-5.7	-1.5	2.7	-1.5	3.2
-2.2	0.0	-0.7	-1.2	0.7	1.5	0.7	-1.7	-7.2
-0.7	2.2	-1.7	-1.7	1.5	-0.2	-3.5	-1.7	-5.9
-0.2	3	-6.4	0.0	2.5	-1.2	1.0	3.2	0.2
0.0	0	0	-2.2	2.0	0.0	-1.0	1.2	-2.5
0.2	-2	0	-1.5	0.2	0	1.2	-1	-2
0.0	2	-2.2	0.0	3.7	0.7	0.5	-0.5	0.7
3.2	0.2	0	0.0	3	0	1.2	-4.4	-6.2
6.7	-9.6	-2.7	0.7	2	0	-5.4	-1.5	0.7
1.0	-9.6	2	7.2	0	4.4	-2.7	-0.2	2.7
0.0	2.5	0.5	1.2	3.2	-6.7	-2.5	-4.2	-1.2
0.0	3.2	4.7	6.9	-0.7	5.7	1.5	3.9	2
0.0	1	-0.5	-2.7	0.7	1.2	-0.2	3.5	1.7
2.0	-2	-2.5	0.3	3.2	2	-5.2	1.5	-1.7
-0.7	0.7	7.9	1.0	1	0	-2.0	0	0
1.0	2.2	0.5	-1.2	2.2	4.4	-3.0	4.7	0.7
-0.7	2.5	0	-1.0	3.7	0.7	1.0	1	1
0.5	0	3.2	-0.7	-0.5	3.5	-1.2	-1.2	1.2
2.5	3.7	3.9	-2.5	4.7	2.7	0.0	0	3
-0.5	1.5	0	2.5	6.4	6.2	-3.5	7.2	1.5

Table A. 17: Individual set-up errors (Δ) acquired from patient 49-51.

Orthogonal Directions (mm)								
Patient 49			Patient 50			Patient 51		
vert.	lat.	long.	vert.	lat.	long.	vert.	lat.	long.
1.6	0	-0.7	-9.1	-3.5	-19	6.2	0	0
-4.7	1.6	0	0.2	0.3	-18.7	8.9	8.1	5.7
0.0	0	0	2.7	-10.9	-3.7	2.5	-2	5.4
0.0	-8.4	-1	1.5	1	1.2	6.4	12.5	3
0.0	1	0.7	-2.2	-8.6	1.5	10.0	-5.3	7.9
-2.0	1	0	4.7	4.2	2.7	5.9	-2	8.9
-3.0	0	3.5	-1.0	-1.2	-2.2	0.0	3.5	2.5
-4.4	4.4	1.7	0.3	-5.3	1.3	4.4	12.3	3
-2.5	0	0	-0.2	-11.3	-0.5	1.5	-2.5	2.5
-2.5	0	0	1.7	2	-17.3	1.0	2.5	1.5
-3.7	4.9	3.5	-1.3	3.3	-18.7	4.0	7.4	0.5
1.2	3.9	-1.5	0.0	2.3	-13.2	0.0	0.5	3.9
-4.4	1	-2	0.1	1.2	-12.8	-4.9	-2.2	-0.7
-5.2	2.2	-0.7	4.6	0	-11.8	-3.7	6.9	-1.0
-6.2	0	9.4	-4.4	-6.7	-13.6	2.2	-5.2	-2.2
-1.5	1.5	1.2	-5.9	-3.6	-12.5	4.4	-10.4	1.7
0.3	0	2.5	-5.3	-3.7	-17.8	-2.0	-3.2	0.5
1.2	0	2.2	1.0	-1.5	-18.5	-1.3	-5.9	0
-6.4	0	0	-0.5	3	-19.7	-2.2	-3.9	-0.7
0.5	2.2	1	0.0	-8.2	-16	-0.7	0	3.3
-1.2	-9.9	1	1.5	-2.2	-16.8	-1.0	-5.4	1
1.5	-1	2.2	-1.0	-3.5	3.5	-0.7	-10.6	1.5
0.5	-0.5	-0.7	-1.3	0.5	3.0	-0.5	-9.4	-0.2
-0.5	1.5	1.7	0.3	-1.3	3.0	2.2	-9.4	2.7
0.0	-10.1	0.5	-1.3	0.2	4.9	0.5	-0.5	1.2
2.0	-10.9	-9.4	2.1	-3	1.2	-0.7	-4.4	0.7
-0.5	-6.4	6.2	0.5	7.2	5.3	-1.0	-16.3	2
-0.7	-6.9	-15.3	-4.6	2.6	5.3	-7.2	-2.5	1.7
-5.2	-4.4	-16.3	-4.4	3.5	2.5	-1.5	8.6	-4.9
5.7	-5.2	14.8	1.0	-1.5	2.5	-1.0	1.2	0.7

Table A. 18: Individual set-up errors (Δ) acquired from patient 52-54.

Orthogonal Directions (mm)								
Patient 52			Patient 53			Patient 54		
vert.	lat.	long.	vert.	lat.	long.	vert.	lat.	long.
-0.5	-5.4	-0.5	-2.0	-0.7	1.2	1.7	-1.7	5.2
0.0	6.9	0.7	0.7	-2.3	3.9	0.0	-0.7	1
-2.2	-3.5	-1	-2.0	-2.7	5.7	1.0	0.7	5.7
-1.0	-4.4	-1.2	0.7	-2.2	4.7	-1.0	0.2	5.2
-7.4	-7.9	3.5	-1.2	-3.2	-1.2	0.2	1.2	3.2
1.0	-3.7	-1.2	-2.9	-4.1	2.9	-2.0	-3	2.7
-1.0	-2.5	-2	-1.5	-0.7	3.2	0.5	-3.7	-1.7
0.0	-1.2	-1	1.5	-4.4	3.2	-1.5	1	0.7
-1.7	-4.4	-2	1.7	-4.9	4.4	3.0	-2.5	5.9
-3.5	-0.2	0.5	1.5	-1.2	1.5	-2.5	2.5	0.7
1.5	1.5	-14.3	-1.5	-2.5	2.5	-3.5	-0.2	1
-2.7	-0.5	0.7	-0.5	-1.5	-0.5	1.0	3.7	3.5
0.2	-6.4	-2.7	3.7	12.3	3.9	-4.2	2	3.2
-3.7	-4.7	-1.5	4.2	-0.2	4.9	7.2	3.5	7.9
0.0	-8.1	-3.5	2.0	2.7	4.7	-4.2	0	2.5
-1.0	-1.5	-0.7	3.9	-0.5	4.9	-3.5	0.5	4.2
0.7	-11.1	0.7	1.2	-0.7	1.7	-1.0	2.7	3
-5.4	-1.2	0.2	2.5	-0.2	6.5	-0.2	6.2	7.4
-0.2	6.1	1.5	0.2	-2	2	-3.2	1.7	4.9
-2.7	6.2	0.5	2.7	0.7	6.5	1.0	-1	5.9
-7.2	1.7	-2.7	1.2	-1	2.2	-2.7	0.2	5.2
-1.7	3.9	2	1.2	-0.2	1.2	-4.4	-1.5	6.4
-3.7	-3.7	2	-1.7	2.2	3.5	-5.7	0.2	2.7
1.7	-3.5	3	0.5	0.5	2.7	-2.7	0.5	7.6
-1.0	-3.2	2.7	-6.4	0.0	0.2	-1.2	2.5	4.9
-2.2	-0.5	1.7	3.0	-0.5	4.7	3.7	2	5
-3.9	-0.2	-0.2	0.0	-0.5	0.0	1.0	-1	8.4
-5.1	-2	0.2	2.2	2	4.7	-4.2	3	5.4
1.2	1	0.7	3.2	0.5	3.9	-1.2	2.7	4.2
-1.0	0.2	3.6	-0.5	-2	3	-1.2	-0.2	3.7